

**POLITECNICO DI MILANO**

Faculty of Industrial Engineering

Master of Science in Mechanical Engineering



Rolling Road System Design for the RuotaVia Test Rig

Relatore: Prof. Giampiero MASTINU

Co-relatore: Ing. Mario PENNATI

Tesi di Laurea di:

Juan Felipe BAQUERO Matr.737630

Anno Accademico 2009 - 2010

# Acknowledgements

The author wishes to express his most heartfelt thanks to his family, for their constant support along the years and especially along this two year abroad experience.

To professors Giampiero Mastinu, Mario Pennati and Massimiliano Gobbi for their patience, guidance and encouragement which made this project possible.

Finally, to Politecnico di Milano and the Mechanical Engineering Department for their enriching Master of Science program.

Juan Felipe Baquero

# General Index

<b>1</b>	<b>Introduction.....</b>	<b>7</b>
	1.1 Objectives	8
<b>2</b>	<b>The RuotaVia Test Facility .....</b>	<b>9</b>
	2.1 The Testing Procedure	15
<b>3</b>	<b>Design Process of the Rolling Road.....</b>	<b>23</b>
	3.1 Designs Considerations	23
	3.2 Stainless Steel Belt Design	25
	3.3 Rolling Road Design with Poly-V Belt	33
	3.4 Selection of the Poly-V Belt	34
	3.5 Transmission System	39
	3.6 Rolling Road Structure	46
<b>4</b>	<b>Externally Pressurized Air Bearing .....</b>	<b>50</b>
	4.1 Introduction to Air Bearings	50
	4.2 Design of the Air Bearing Pad	54
	4.3 Air Bearing Test	58
<b>5</b>	<b>Conclusions.....</b>	<b>68</b>
	<b>Bibliography .....</b>	<b>70</b>
	<b>Figure References.....</b>	<b>71</b>
	<b>APPENDIX 1.....</b>	<b>72</b>
<b>1</b>	<b>Belt Support with Rolling Cylinders .....</b>	<b>72</b>

## List of Figures

Figure 1 - Rotating Drum.....	10
Figure 2 – RuotaVia’s Drum, Motor and Gearbox.....	12
Figure 3 - RuotaVia Testing Example.....	16
Figure 4 - Cleats Cross Sections .....	17
Figure 5 - Detail of Actual Opposite Wheel Support.....	18
Figure 6 - Suspension Parameter Measurement Machine (SPMM).....	19
Figure 7 – Rotating Drum Tire Testing Machines .....	20
Figure 8 - MTS Flat-Trac III CT (Cornering And Traction).....	21
Figure 9 - Windshear Inc. Rolling Road .....	22
Figure 10 – Beams Limiting the Available Space for Rolling Road .....	24
Figure 11 – 3D model of the RuotaVia and the Proposed Stainless Steel Rolling Road .....	25
Figure 12 - RuotaVia Stainless Steel Belt Rolling Road Scheme .....	26
Figure 13 - Driving Pulley Forces.....	28
Figure 14 – Power Transmission for Steel Belt. Belt Section and Pulley .....	30
Figure 15 - Belt Tracking Defect .....	31
Figure 16 - Pulley Axis Adjustment and Forced Tracking.....	31
Figure 17 - POLY-V belt L type section.....	34
Figure 18 – L Section Belt and Pulley Dimensions .....	35
Figure 19 - Rolling Road Basic Dimensions.....	35
Figure 20 - Resultant force on Pulleys .....	36
Figure 21 - Resultant Force on Pulleys .....	37
Figure 22 - Air Bearing Support for Rolling Road Belt.....	38
Figure 23 - Belt Selection for a given Power and RPM.....	40
Figure 24 - Angles of Belt and Pulley.....	44
Figure 25- Loads at the Rolling Roads Main Shaft.....	45
Figure 26 - Rolling Road Render .....	46
Figure 27 - Rolling Road without the Main Belt.....	47
Figure 28 - Rolling Road Structure Main Components.....	47
Figure 29 - Angular Contact Bearings .....	48
Figure 30 - SKF Bearing Housing Modification.....	48
Figure 31 - Rubber Belt Rolling Road in the RuotaVia Test Rig.....	49
Figure 32 - Porous Media Air Bearing.....	52
Figure 33 - Radial and Flat air bearing .....	52
Figure 34 - Orifice Flow Meter Scheme .....	54
Figure 35 - PK Belt Profile .....	59
Figure 36 - Model Air Bearing for Test .....	60
Figure 37 - Air Bearing Experimental Test Setup.....	61
Figure 38 - Air Bearing and Belt Supporting a Steel Mass .....	62
Figure 39 - Experimental Air Bearing Performance .....	63
Figure 40- New Way Flat Pad Air Bearings Ideal Load .....	63
Figure 41 - New Way Flat Pad Air Bearings Efficiency.....	64
Figure 42 - Air Bearing Definite Concept.....	66
Figure 43 - Detail of Orifice Location .....	67
Figure 44 - Alternate Belt Supporting Method with 10 Supporting Cylinders .....	72
Figure 45 - Rolling Cylinders Assembly Detail.....	73
Figure 46 - Rolling Road Support with 7 Rotating Cylinders.....	75

## List of Tables

Table 1 - Rotating Drum Natural Frequencies .....	11
Table 2 - Ruotavia Drum and Concrete Box .....	12
Table 3 - RuotaVia Test Rig Driving System .....	14
Table 4 - Ruotavia Braking System .....	15
Table 5 - Stainless Steel Belt Dimensions.....	27
Table 6 - Transmission Belts Main Parameters.....	43

## Abstract

The behaviour of road vehicle suspension systems has a considerably important effect over the overall performance, controllability, safety and comfort of modern vehicles. As a consequence of its importance, specific testing procedures and facilities have been developed, allowing a deeper understanding of the behaviour of vehicle suspension systems and tires. The RuotaVia Test Rig, located at the Laboratory for the Safety for Transport (L.A.S.T.) of Politecnico di Milano, allows the study of the vibration performance of suspension systems, by introducing a cyclic disturbance to a single wheel rotating over a steel drum. The necessity of further developing the vibration analysis requires a more advanced simulation of the suspension's behaviour, and therefore introducing the rotation of an additional wheel during testing became a necessity. A rolling road system was specifically designed to fit the requirements of the RuotaVia facility, allowing the simultaneous rotation of both wheels (left and right) of a single vehicle axle. In order to support the second wheel some design alternatives were studied and their feasibility was analyzed. Finally an externally pressurized air bearing was designed to pneumatically support a rotating POLY-V rubber belt over which the vehicle tire rotates. The bearing supports the load over the rubber belt while significantly reducing the friction and the required driving power of the rolling road system.

**Keywords:** rolling road, RuotaVia, suspension system testing, air-bearing.

# Chapter 1

## 1 Introduction

Modern vehicle suspension systems are a fundamental part of road vehicles due to their important effect over the vehicle's behavior, safety, control, handling and comfort. Being the suspension the direct link between the road and the vehicle frame, an adequate tuning of the system is mandatory in order to achieve the desired response and control of the vehicle while offering comfort according to the type of vehicle and its purpose. A good suspension system must be designed to provide an adequate and constant contact between the road and the tires, while adequately dissipating the energy introduced by the irregularities of the road.

A modern suspension system is composed of many different elements, and as a consequence its overall behavior and response depends on the complex interaction between components such as tires, springs, dampers, torsion bars and even the chassis of the vehicle. In a suspension system, springs (either coil or leaf type) are used to guarantee the contact of the wheels with the road, allowing the tires to move up and down while following the irregularities of the road. On the other hand, dampers (also known as shock absorbers), help to gradually dissipate the energy of the springs to reduce the motion of the chassis. According to the use of the vehicle (road vehicle, off road, racing, working vehicle etc) an adequate tuning between the stiffness of the spring and the type of shock absorber must be found. In example to limit control the displacement of the suspension, it is possible to use very hard springs, or use soft springs acting simultaneously with dampers. Even more, modern suspension systems use sway bars (torsion bars) that connect the opposite (left-right) wheels of an axle, and so the response of the vehicle and its suspension has a complex dynamic involving many elements and is therefore very hard to predict it or simulate it numerically.

Considering the complexity of the interaction between the many variables affecting the behavior of a vehicle suspension system, it is not simple to understand the actual behavior of a suspension and determine if it actually satisfies the design requirements. Therefore characterizing the behavior and response of a suspension system is not an easy task, and so an adequate suspension testing method must be able to adequately simulate the real interaction between all the components, in order to obtain accurate results.

As a result of the importance of studying and understanding the behavior of vehicle suspension systems, many different testing facilities and devices have been developed to test tires and/or suspensions in order to adequately characterize their behavior under controlled environments, speeds and loads. Among the available suspension testing systems, we find the RuotaVia Test Rig located at the Laboratory for the Safety of Transport (L.A.S.T.) of Politecnico di Milano. This thesis project intends to propose a design solution for a rolling road system able to fit the RuotaVia facility in order to further develop the capability of the facility of adequately studying the vibration behavior of vehicle suspension systems by providing a way to support and make rotate the tire at the opposite side of the shaft of the tire being tested. In this way, more accurate results will be obtained during testing, as the vehicle behavior will be simulated in a much more adequate way, since more elements of the suspension will be working as they would normally do during real operation, and not anymore unrealistically constrained to fit the test rig, since both tires will be rotating.

The following chapters of this document contain detailed information about the RuotaVia test rig and its main characteristics, different aspects about vehicle suspension testing, and of course the design process and relevant calculations that were developed for the different possibilities that were studied to arrive to the final proposed design solution.

## 1.1 Objectives

This project intends to study the possible design solutions for a rolling road system specifically designed to fit and perform in the RuotaVia test rig. The rolling road must give support to an average size road vehicle wheel and to the forces generated due to the weight of the vehicle, while making the wheel rotate at an equal speed to that of the tire over the rotating drum, in order to simulate the vehicle's motion. The proposed solution will be based on the state of the art designs for engineering problems of similar characteristics, adapting them to the particular characteristics and limitations of this project. By analyzing the positive and negative characteristics of the possible solutions, the most adequate solution will be developed and proposed for implementation at the test facility.

The most feasible design according to the economical, performance and manufacturing limitations will be proposed, which must be able to support the wheel and make it rotate while not interfering with the normal operation of the RuotaVia test rig. The system must provide a smooth drive to the tire, matching the RuotaVia drum tangential speed while testing in order to provide an accurate simulation of the suspension system behavior and response.



## Chapter 2

### 2 The RuotaVia Test Facility

The vibration behavior of a vehicle suspension depends on a number of variables with complex interactions in between them. The type of tires, springs, dampers, the structure of the suspension and of the chassis, all have an important effect over the actual behavior of the vehicle. Given the number of variables affecting the vibration response, it results quite unreal to think about successfully developing a valid mathematical model that could adequately allow the engineer to understand how a vehicle will perform by means of simulations and simplified mathematical models. Given the complexity of the problem, simulations have proven inadequate or insufficient to analyze the problem and therefore methods based on the direct measurement of the forces and moments to which the suspension elements and tires are subjected when excited have been developed.

The RuotaVia is an indoor testing facility, built at the Laboratory for the Safety for Transport (L.A.S.T.) at the Bovisa campus of Politecnico di Milano. The rig was built in order to carry out testing on the vibration behavior of vehicle suspension systems and/or the assessing tire characteristics. The testing facility operation is based on a 2.6 meter diameter rotating steel drum, which provides a running contact surface for the tires. The contact between the tire and the rotating drum makes the tire rotate, and so the tire's rotational speed is controlled by changing the drum's rotational speed. The rotating steel drum and most of the structure that supports the RuotaVia were located under ground level, so only a small fraction of the drum emerges from the ground level thanks to which the space available over the drum is generous, and makes it possible to mount over the test rig a single independent suspension, meaning just one of the tires of the vehicle, up to a complete vehicle of medium size. However, given the size of the drum, it is only possible to drive and test one of the vehicle's wheels, and so, the rest of the vehicle's suspension and frame must be adequately constrained.

The RuotaVia was designed to serve not only as a test rig for vibration analysis of suspensions, but also as test rig for tires. Therefore, it was designed to be able to support high loads in different directions in order to simulate the forces a tire has to support during different driving conditions. The test rig is then capable of holding maximum loads of 100 kN in the radial direction, 100 kN in the tangential and 100 kN in the lateral direction (axial respect to the drum). The

understanding of the forces to which the tires and the suspension are subjected under steady state and dynamic conditions became important for the analysis and investigation of vehicle rollover. It was then that the necessity of developing a method to study the vibration and forces of these systems became increasingly important. These necessities lead to a feasibility analysis of a test rig able to satisfy the testing conditions requirements. Possible solutions such as flat tracks systems and big rotating wheels were considered. The implementation of a big rotating wheel (with a diameter over 4 meters) was an interesting alternative for the possibility it offered of simulating flat surface conditions (due to the large radius), but later proved unfeasible since it resulted difficult to give such big wheels the required stiffness. Finally, a test rig based on a smaller diameter drum was implemented, since this option offered the best compromise between the considered parameters such as speed, stiffness and radius of the surface. The RuotaVia test facility may be used for testing tires, suspension and braking systems of road vehicle or other systems of similar size.

The design process of the RuotaVia test rig was guided by some objectives related to the required performance of the rig in order to achieve adequate testing results. Among the considered parameters, the most relevant that must mention were: high speed testing, possibility of testing different types of systems (i.e. motorcycles and road vehicles), tire testing passing over cleats, testing of complete or subsystems, testing of braking devices and tires, and fatigue testing of wheel rims.



**Figure 1 - Rotating Drum**

The rotating steel drum is the fundamental element of the RuotaVia test rig. The drum was built with a 100mm thick one piece steel forged ring, which serves as the outer part of the drum, and therefore provides the contact surface over which the tires rotate while testing. The outer ring was then connected to a central hub

using two side disks. Additionally, 16 plate shaped spokes were used to increase the lateral stiffness of the drum. The spokes were welded to the central hub and the lateral discs but not to the outer ring in order to avoid the deformation and undulation of the ring's surface while rotating at high speeds, which must be as rounded as possible to simulate a flat road. Once the drum was welded, a stress relief annealing process was performed, which was then followed by a finishing process in the turning lathe to guarantee dimensional precision. The drum was then finished by fitting it to the shaft by means of two friction cone clamping units. The finished steel drum has a width of 550 mm and a mass of 5500 kg.

<b>Rotating Steel Drum Natural Frequencies</b>		
<b>Vibration Mode</b>	<b>Frequency [Hz]</b>	<b>Type of Vibration Mode</b>
1	95	First shaft bending mode in the horizontal plane
2	95	First shaft bending mode in the vertical plane
3	152	First disks bending mode
4	171	Second shaft bending mode in the horizontal plane
5	171	Second shaft bending mode in the vertical plane
6	277	Second disks bending mode

**Table 1 - Rotating Drum Natural Frequencies**

Considering the characteristics of the testing to be developed on the rig, special attention was given to the vibration modes of the drum and the entire structure of the test rig, so that the frequency range of interest during testing would not be affected by the vibration modes of the rig itself. The foundations and structure of the test rig were carefully designed in order to avoid the transmission of vibration to nearby structures and reduce undesired noise during the measurements. The drum and the driving systems are supported by a concrete and steel frame, whose structure was modeled by means of finite elements and the natural frequencies were set over 100 Hz. The design of the drum and the studying of its performance and behavior were based on a finite element analysis (FEM), in which the drum was simulated under the effect of centrifugal forces. The FEM analysis was developed by simulating a peripheral (tangential) speed of the drum of 450 km/h, while loaded with a 10 kN compression load, a 12 kN longitudinal load and a 12 kN axial force, all of them applied at the top of the drum [2] where the vehicle's tire should be located during testing. The

analysis determined the highest stresses at the drum occur at the welding between the lateral discs and the outer ring (Von Misses stress of around 182 MPa).

RuotaVia Test Rig		
Concrete Box	Dimensions	3.85 x 6.90 x 4.30 m
	Isolation	Stiffenite
	Mass	140 tons
Drum	Max. Speed	440 km/h
	Diameter	2600 mm
	Width	550 mm
	Mass	5500 kg
	Polar Moment of Inertia	5660 kg m <sup>2</sup>

**Table 2 - Ruotavia Drum and Concrete Box**

Most of the components and structure of the facility are located under ground level, thanks to which the entire structure is supported by a very stiff and isolated concrete box (140 tons), which in addition to a structure of double-T steel beams give support to the drum, the motor and the gearbox, Thanks to which the natural frequencies of the test facility are high enough as to not affect the measurements over the suspension, or transmit vibrations to nearby elements.

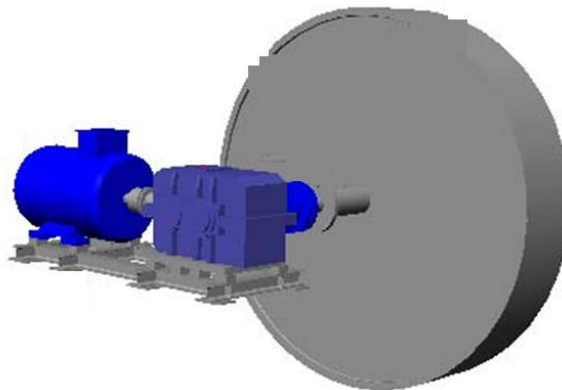


**Figure 2 – RuotaVia’s Drum, Motor and Gearbox**

The rotating drum is driven by a 160 kW four pole asynchronous electric motor, which is connected to an angular double speed gearbox by means of flexible joints. The gearbox has a low speed ratio of 15:1 and a high speed reduction ratio of 3:1. With this motor and transmission configuration, it is possible to drive the drum up to a maximum tangential speed of around 440 km/h with the

high speed gear ratio (the speed of the drum is measured with a 4096 point encoder). On the other hand, the low speed ratio makes it possible to maintain a constant rotational speed of the drum at low speeds even when the drum is loaded simulating the weight and forces generated by an average size vehicle (a vertical force around 10 kN with a certain steering angle), which is important while testing.

The selection of the electric motor required to drive the drum was based on the calculation of the power required to maintain a constant rotational speed. Consequently, the different sources of power loss were considered to determine the total required power. Three main sources of power loss were identified: those caused by the steer angle, those caused by the wind, and finally the rolling losses. The steer angle losses  $N_s$  were calculated based on the ratio between the lateral force and the vertical load  $\mu_y$  (which was assumed as 1.3 for this case), the vertical load  $F_z$ , the steer angle  $\alpha$ , and the drum's tangential speed  $V_h$ . The steer angle power losses were then calculated as:

$$N_s = \mu_y F_z \sin(\alpha) V_h$$

In a similar way, the rolling losses of the tire  $N_r$ , which are much smaller to the steer angle losses, were calculated [2] in a simplified way as caused by a tangential force in the drum equivalent to 2% of the vertical force:

$$N_r = 0.02 * F_z \sin(\alpha) V_h$$

During the design process, the calculations were based on a 5 degree steer angle  $\alpha$ , a tangential speed of the tire  $V_h$  of 400 km/h (112 m/s), and a 10 kN vertical load  $F_z$ . With those parameters, the steer angle losses reached 127 kW, while the rolling losses added 22 kW to the total required power. Besides these losses, an additional 3 kW loss was considered for the losses associated to the resistance caused by the air flowing around the drum and opposing to its rotation at high speeds. It was therefore necessary to select at least a 152 kW motor, in order to achieve the desired performance.

Besides the previous analysis of the power requirements at maximum speed, the calculations for the required power of the motor were confirmed by considering a second experimental procedure, in which the power loss is calculated referred to the lateral versus longitudinal forces on the tire, while rotating at a steady state speed. Considering the extreme case where the longitudinal force equals the vertical one while rotating at a low and steady state speed  $V_1$  (set as 50 km/h = 14 m/s), the power required to maintain a constant tangential speed would be:

$$N_l = F_z V_l = 10\,000 * 14 = 140\text{ kW}$$

And therefore, a 160 kW (around 215 hp) electric motor would also be enough to carry out this test. At the low rotation speed conditions used for the second experimental procedure, the power losses due to the wind and the rolling of the tire may be neglected.

RuotaVia Test Rig Driving System		
Motor	Type	Electric Asynchronous 4 poles
	Power (Max. Continuous)	160 kW    Cos $\phi$ 0.85
Transmission	Type	2 speed gearbox
	Low Speed Ratio	1:15
	High Speed Ratio	1:3

**Table 3 - RuotaVia Test Rig Driving System**

A superstructure was also designed in order to give adequate support and constrain when testing single tires on the rig, while offering flexibility in the setup of the rig to set the suspensions in wide variety of positions with different loads. The superstructure is a steel frame with which is possible to apply a vertical force up to 100 kN and move the tire along the vertical and axial. It also allows the rotation and setup of the steer and camber angles. The camber may change in the range of +6 to -80 degrees, while the steer angle can be varied between +25 and -25 degrees. The rotation angles of the superstructure are controlled by bearings powered by electronically controlled brushless motors, so all the parameters are precisely controlled. Since the motions of the superstructure are electronically controlled, it is possible to set different trajectories for the tire while rolling over the rotating drum. However, for the purpose of this project, the superstructure is not further considered, since this document focuses on the implementation of the rolling road, whose use is for different kind of suspension testing, were an entire suspension is mounted on the test rig, and therefore the super structure is not required.

Considering the high rotation speeds that can be achieved by the drum, and its high inertia (weights 5.5 tons), the RuotaVia test rig was equipped with two braking systems. The main braking system is a self ventilated Brembo disk with a diameter of 430 mm operated by a pneumatic Knorr Bremse caliper (SB7112 radial 24"). This braking disc was located in the main shaft of the drum, at the opposite side from where the gearbox is located. When operating at the maximum input pressure of 6 bar, this braking system is capable of applying a 1200 N-m torque to the drum's shaft, which may decelerate the drum from its maximum tangential speed of 440 km/h to zero in just about 50 seconds.

RuotaVia Test Rig Braking Systems		
Main Brake	Type	Pneumatic disc brake
	Disc	Self Ventilated diameter 430mm Brembo 09.7380.20
	Caliper	Knorr Bremse SB7112 radial 24"
Speed Control Brake	Type	Hydraulic disc brake
	Disc	Brembo Self Ventilated diameter 380mm
	Caliper	2 hydraulic Brembo Calipers

**Table 4 - Ruotavia Braking System**

An additional braking system was also fitted to the drum's shaft, but this time located between the gearbox and the drum itself. This secondary braking system is also a self ventilated disc, but has a slightly smaller diameter (380 mm) and is operated with two hydraulic calipers. These two calipers of this smaller braking system are precisely controlled electronically. The electronic control can act on the break up to a frequency of 50 Hz, and so it is used to control the rotational speed of the drum with high precision during testing.

## 2.1 The Testing Procedure

The first step on the testing procedure at the RuotaVia test rig is the assembly of the suspension to test on the rig. If a single tire with its suspension is to be tested, it is necessary to use the previously described superstructure to constrain the elements. Once again, given the scope of developing a rolling road for the facility, we focus on the case in which at least a complete axle (front or rear) with its left and right tires is to be used during the testing, in which case the vehicle frame must be adequately constrained. One of the tires must be located over the drum, and the other must be adequately supported. The actual configuration of the test rig does not have a system to support the tire at the opposite side of the axle of the tire over the rotating drum. The following pictures illustrate a typical testing case of a rear axle mounted in the test rig. The picture at the left side shows the right side rear tire, properly located over the rotating drum. Meanwhile the picture at the right shows the left rear wheel, which as can be seen, is simply supported over some plates, but may not rotate. We must notice that all the suspension system is supported by the blue structure, which loads the springs and dampers to simulate the weight of the vehicle.



**Figure 3 - RuotaVia Testing Example**

Once the suspension is adequately positioned, with the tire in contact with the drum and the necessary constraints, like observed in the previous images, the test rig can be used to analyze the vibration performance of the suspension. The testing is done by imposing a periodical excitation to the suspension by means of cleats attached to the surface of the rotating drum. In this way, every turn of the rotating drum, the wheel runs over the cleat and energy is introduced in the suspension system. The excitation generated in the suspension by the cleat at the drum, applies forces and moments to the different elements of the suspension which are measured and analyzed.

The excitation of the suspension occurs every time the wheel passes over a cleat which is attached to the outer surface of the drum. Therefore, the characteristics of the excitation such as the amplitude can be varied by changing the dimensions of the cleat (height and width), while the frequency can be changed by either changing the rotating velocity of the drum or the number of cleats bolted to the drum's surface. Even though the facility is big enough to fit an entire road vehicle, the testing and measurements may only be done at the wheel rotating over the drum, which is at the moment the only rotating tire. The experimental procedure, as developed in [1] consists of exciting the system with cleats of different cross section geometries while rotating the drum at different speeds up to a maximum of 100 km/h. Figure 4 shows the cross sections of the cleats used by [1], from which we can notice how different heights and widths may be used to excite the system in different ways.



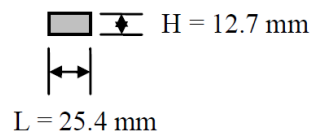
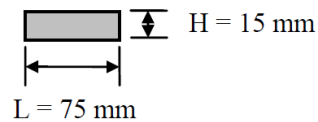
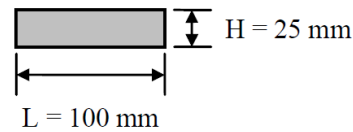


**Figure 4 - Cleats Cross Sections**

In order to develop the vibration performance testing (as described in [1]), it is necessary to instrument the suspension elements in order to be able to measure the forces. In this case, the instrumentation is based in six-axis load cells located at each joint of the suspension's structure. The specially created load cells make possible the measurement of 3 forces and 3 moments in each joint. In addition to the load cells, also infrared cameras are installed and used to measure the displacements of the center of the tire in the different directions, by following the position of some marks placed in the wheel rim.

For an adequate testing, suspension systems require a warm up process, in order to take the different elements to their actual operation temperature. This is important since many suspension elements change their behavior with temperature, such as the dampers due to the heating of the oil, and the tires which increase their temperature due to the continuous deformations they suffer. The warm up process therefore consists of allowing the suspension to work for a number of kilometers at a moderate speed (i.e. 5 km at 15 km/h). Once the warm up is concluded, the instruments are set to zero to begin the actual measurements of forces and displacements. The testing procedure is then started by applying a ramp shaped function to the rotational speed of the drum until reaching a constant maximum value. The acceleration of the drum is set to a low value ranging from  $0.04$  to  $0.08 \text{ m/s}^2$ , so that the speed variation can be neglected when the tire passes over the cleat. In order to determine the maximum speeds and accelerations to use during the actual testing, a previous testing must be carried out in order to determine the speeds and accelerations that do not significantly change the measured forces according to the cleat geometry. For example, maximum speeds of 50 and 80 km/h have been determined for the 25 and 15 mm high cleats respectively. The testing process is concluded by

allowing the suspension to pass repeatedly over the cleat, in order to obtain sufficient data as to perform averaging and eliminate any white noise present in the data.

Once the testing part is concluded, the data analysis is performed. The data is separated in order to develop a “constant speed analysis” and a “varying speed analysis” which obviously refer to the data obtained while the drum is rotating at a constant speed, and when it is in the acceleration phase respectively. The constant speed analysis offers very clear information about the vehicles vibration behavior, since an averaging process can be easily performed to eliminate the noise present in the measurements. A typical testing procedure at the RuotaVia gives the direct measurements of the drum speed, the 3 dimensional components of the acceleration of the wheel’s center, plus the 3 forces and moments of each suspension joint, and the force along the steering arm. In addition, the displacement of the wheel’s center can be determined by using the infrared cameras. Using all the measure data it is possible to calculate the suspension’s damping coefficient by applying the Hilbert’s Transform.



**Figure 5 - Detail of Actual Opposite Wheel Support**

As previously mentioned, the actual configuration of the test facility is only capable of rotating one of the wheels of the vehicle. Figure 5 shows the detail of how to the date, the opposite wheel is being supported over some fixed metal plates, when an entire axle is mounted on the rig. However, the actual behavior of a single suspension is closely coupled to the behavior of the rest of the vehicles suspension system. In example the measurement of the forces and vibrations at the wheel over the drum are strongly dependant on the behavior of the other wheels of the vehicle, since they are directly linked by the chassis and

a sway bar in many cases. It was therefore, the need of more accurate testing results that led to the development of this thesis project, in which a design proposal for a rolling road was developed in order to allow the rotation of the tire at the opposite side of that one being tested. Therefore the objective is to design a system to support the wheel as seen in figure 5, but making the wheel rotate at the same velocity as the opposing wheel rotates over the RuotaVia drum while testing. The implementation of the proposed design will allow a more realistic test of the suspension systems, as it will be possible to simultaneously rotate the left and right wheels of a single axle.

## 2.2 State of the Art: Tire and Suspension testing

Suspension systems' testing has been developed for many years in the automotive sector. Among the companies working in the testing industry, the ABD Company (Anthony Best Dynamics) is one of the leading brands, and has been developing testing machines for suspension systems for over 25 years. Known as *Kinematics and Compliance Measurement Machines*, this kind of test rigs are useful to study the suspension's characteristics under quasi-static conditions, by measuring the kinematic characteristics of a suspension design in order to understand the vehicle's behavior. Among ABD's most widely known systems, are the known as *Suspension Parameter Measurement Machines* (SPMM). These testing machines are very useful to understand the characteristics of the complete suspension system of a vehicle, since it is designed to hold the complete car, not only the suspension system itself.



**Figure 6 - Suspension Parameter Measurement Machine (SPMM).**

Testing machines such as the SPM are based on electric actuators, which act under the wheels simulating forces and displacements caused by the road's surface imperfections. In the most advanced machines some actuators act over the vehicle's frame to simulate the movement of the chassis while driving. However, these machines do not allow the rotation of the wheels, so the effect of the rotation and deformation of the tires is not considered during the tests. SPM testing machines may be found in different configurations, ranging from those that may only fit a single axle with its two wheels, to those able to hold the complete vehicle and are even capable of calculating its center of gravity by fixing it to a central plate and performing some determined movements with the entire car.

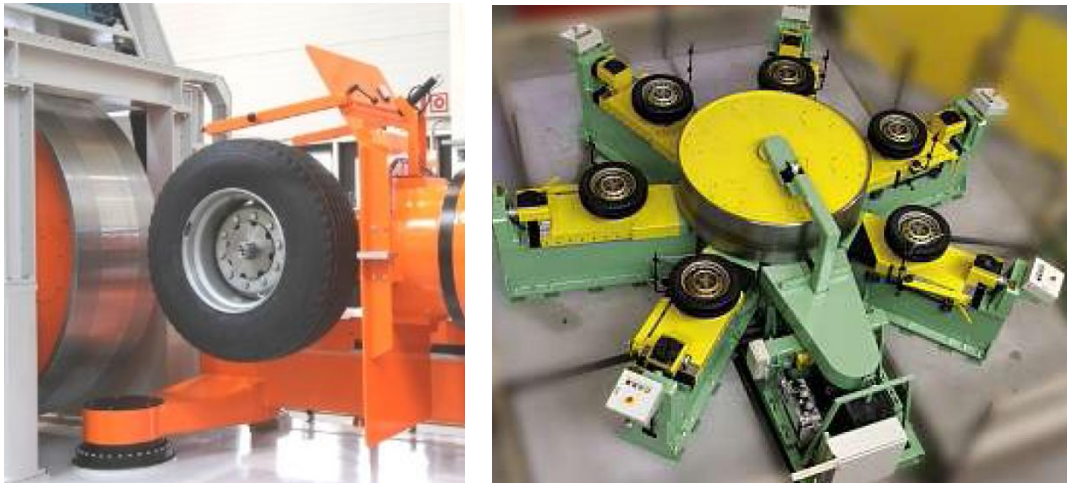


**Figure 7 – Rotating Drum Tire Testing Machines**

Considering the difficulty to create a test rig adequate both for suspension and wheel testing, different approaches have been developed to test tires, most of them based on rotating drums or rolling roads. Figure 7 shows a typical modern testing machine for tires based on a rotating drum. These machines are able to measure the forces and moments the tire experiences while rotating at different speeds and changing different parameters such as the slip angle and the camber. By the nature of these machines, we notice that it is not possible to test suspensions in them, and of course a entire car is impossible, since it would be necessary to mount the suspension in a horizontal way. This same type of testing machine is frequently used to simulate the tire thread wear, by using plates on the drum with different textures to simulate the road's surface. The advantage of this type of rotating drum testing machines, Is the possibility of testing more than one tire at the same time, using the different sides of the drum, which can be a great advantage when performing long lasting tests.

Modern rolling roads are mostly built with stainless steel belts which offer a good strength to weight ration, are economical, may operate in a wide temperature range, have optimal wear resistance and require low maintenance since their lifecycle is usually very long. According to particular needs, steel belts may be produced with different surface finishes such as silicon, Polyurethane or Teflon. Besides the good performance of the stainless steel belts, the production process of them makes it possible to manufacture them in a wide range of sizes with very good accuracy and repeatability. Besides the good performance obtained with metallic belts, they offer the possibility to install sensors under the flat belt, which can be useful to measure different parameter of the vehicle such as the aerodynamic downforce produced by the vehicle (when testing inside a wind tunnel) or the pressure distribution of the tires on the road. For smaller applications with simpler requirements, rubber belts may be used instead of steel, offering a cheaper and simpler solution however with some restrictions in the performance in terms of operation speed, wear and friction.

Therefore, rolling roads are mostly used on systems intended to test tires, and in the last years they have been also implemented inside wind tunnels for more accurate simulations of vehicles performance. Previously, wind tunnel testing was done with the wheels in a stationary position, but the effect of the rotation of the tires and the motion of the road relative to the car usually has a great influence in the aerodynamic behavior of cars. Therefore, rolling roads are a must in state of the art wind tunnels.

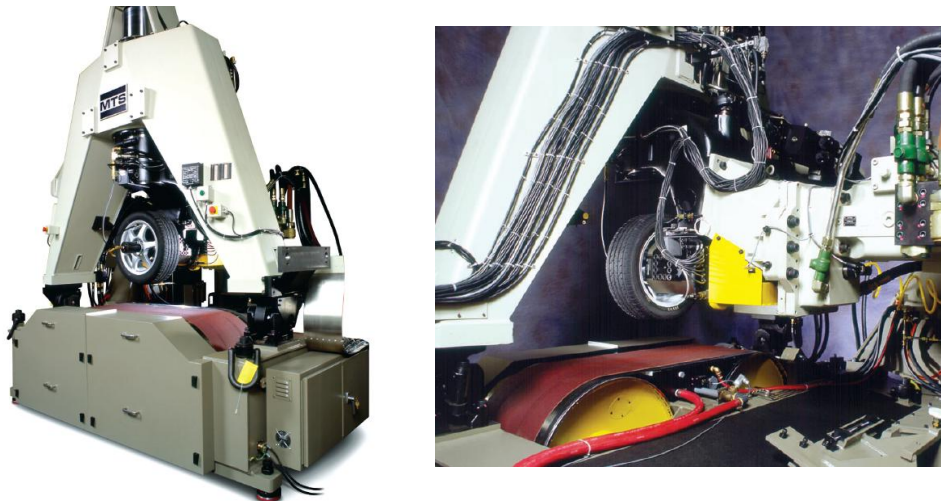


**Figure 8 - MTS Flat-Trac III CT (Cornering And Traction)**

Among the companies working on the tire testing market, MTS is a leading brand which been offering state of the art rolling road systems, sold as FlatTrac® for around 30 years. Most of these *Flat-Trac* systems are used for



testing tires while measuring the forces and moments they must support in different simulated driving conditions. Among the most advanced machines of this type there is the *Flat-Trac LTR* system, designed for testing tires for light trucks, SUV's and racing cars. This system may achieve a maximum speed of 200 mph while subjected to vertical and lateral forces of up to 30kN. So this type of testing machines is very useful to determine the cornering forces to which a tire is exposed, but cannot be used for studying the behavior of suspensions. As seen in the image, Flat-Trac systems consist on a rotating belt that drives the wheel, and a structure around the belt used to support the tire and the instrumentation required for the measurements.

One of the biggest rolling roads built by MTS is located in the United States, belonging to Windshear Inc which was inaugurated in September of 2008. This rolling road, located inside a wind tunnel, is able to fit full-scale vehicles in its single belt system (3 meters wide and 9 meter distance between the rollers), and simulate speeds of up to 290 kph (180mph), and measure the downforce created by the car by means of pressure sensors located under the belt. This type of rolling road is meant to be used for high performance vehicles such as racing cars, in which the air flow under the car has an important effect.



**Figure 9 - Windshear Inc. Rolling Road**

The state of the art of tire and suspension testing machines shows that the characteristics of both types of testing have very different characteristics, and therefore machines for testing tires and suspensions have been mostly developed separately, which is not the case of the *RuotaVia*, where both testing approaches can be developed under certain parameters. We can therefore outline the importance of the *RuotaVia* test rig, which being designed with the multiple purpose of testing suspensions and tires, becomes a unique engineering approach to the tire and suspension testing problematic.

## Chapter 3

### 3 Design Process of the Rolling Road

The design process of the rolling road was approached by studying two possible solutions according to the performance required by the rolling road at the test facility. The first approach was a stainless steel belt rolling road solution, inspired by the state of the art rolling road systems available in the market for tire testing. This solution was analyzed considering its capability of reaching very high speeds, supporting high loads and providing a long expected life. However, the steel belt design approach resulted somehow complicated to build due to its big overall dimensions, which could hardly fit the available space in the RuotaVia test rig. The design process was then continued with the analysis of a simpler and smaller design solution based on a Poly-V belt rolling road supported pneumatically so it could hold the load of the tire. The Poly-V belt was at the end considered as the most adequate solution for the performance requirements and limitations, due to its relative simplicity and construction feasibility. The following chapters present a detailed description of the design process and considerations for the different aspects of the rolling road.

#### 3.1 Designs Considerations

The RuotaVia testing facility was originally designed and built to drive a single wheel, and therefore test a single suspension of a vehicle. However, the need of more accurate testing results made it mandatory to use the complete suspension system during testing. The use of a complete axle or vehicle during the testing requires the implementation of a system to support the opposite wheel, since for these cases the superstructure cannot be used, and even more, the opposite wheel must rotate making the wheel spin as the tire rolling over the steel drum. Since the RuotaVia's structure was not intended to support a second wheel, the available space for the implementation of the rolling road is very limited, especially due to the double T beams that cross the area of interest as seen in figure 10.

Besides the limitation of the space for the rolling road, the new elements for the test facility must not affect the original design of the test rig, since any significant changes on the original structure may affect the stiffness and the natural frequencies of the system which have been carefully set at frequencies

over 100 Hz, to avoid interference with the range of frequencies of interest during the testing. Even more, given the multiple applications of the test rig for different types of testing, the implemented rolling road should offer the possibility to change and adapt to different vehicle sizes and weights, or even to remove it if necessary, so flexibility is fundamental aspect.



**Figure 10 – Beams Limiting the Available Space for Rolling Road**

In belt rolling roads, the load of the tire is located in the middle of the span between the pulleys. This geometry of the system requires the implementation of a supporting surface to counteract the vertical load applied to the belt by the tire which otherwise would rapidly damage the belt, since belts are not designed to be subjected to loads perpendicular to their surface. This aspect of the design results of particular interest, since the friction between the belt and the support is the main source of power loss. Therefore the required torque to drive the belt is proportional to this friction force, considering that the tire rotates freely over the belt and therefore has no significant effect.

Given the importance of the supporting method over the overall rolling road performance, the smallest possible friction coefficient between the belt and the supporting surface must be achieved, also considering the fact that high temperatures might arise in that region. The first approach toward reducing the friction at this zone was by considering the use of low friction coefficient materials such as Teflon or UHMW plastic with which dynamic friction



coefficients as low as 0.04 may be achieved, while causing no damage to the belt, but then, the wear of the components would become an additional factor to consider, besides the high temperatures that could arise in the belt rotating at high speeds.

Given the complicate scenario related to the use of low friction coefficient materials, a more sophisticated approach was taken consisting on the pneumatic support of the belt by means of an externally pressurized air bearing. Under ideal conditions, air bearings may reduce friction between parts to zero by creating an air film in the gap between the two surfaces of interest. However, very strict tolerances and control of the air gap are required to achieve a zero friction coefficient. Air bearings not only greatly reduce friction, but also work with no wear since the surfaces are not in direct contact, reasons for which they are becoming very useful for applications that require high precision.

### 3.2 Stainless Steel Belt Design

Stainless steel belts are the state of the art solution for high performance rolling roads. Among the most important advantageous characteristics of metal belts, are the high strength to weight ratio, which is important considering the high speeds and stresses to which the system will be exposed. Durability is another important advantage of metal belts, even when exposed to high temperatures or aggressive environments. Metal belts operate without the need of lubrication, so the working environment is clean. Further advantages of metal belts are their smooth operation, the fact that they are not stretchable and their construction which can be done with tight tolerances than those applicable for rubber belts.

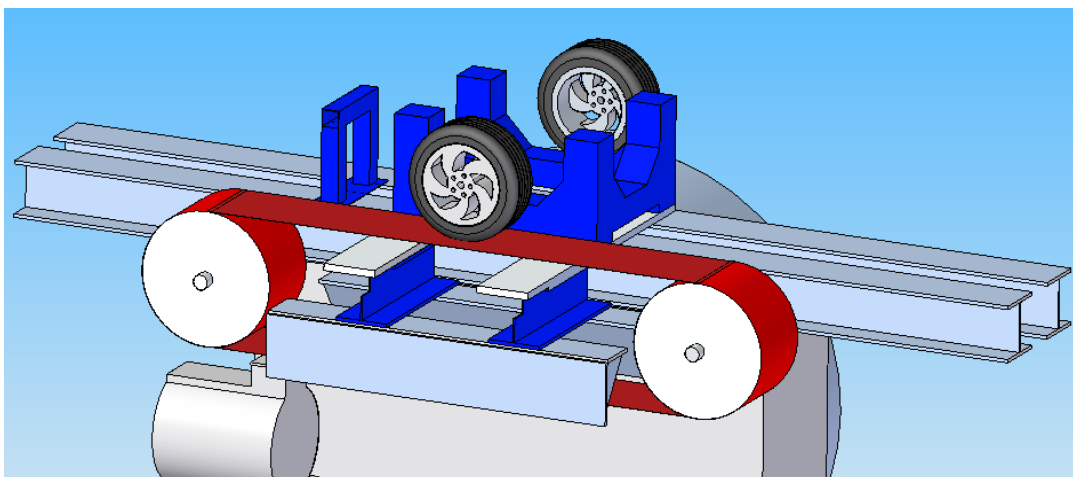


**Figure 11 – 3D model of the RuotaVia and the Proposed Stainless Steel Rolling Road**

When designing belt systems, it is desirable to use the least amount of pulleys, and for the case of metal belts, the use of big diameter pulleys and high length-to-width belt ratios is desired in order to obtain a longer life cycle for the belt, according to the theory presented by the manufacturers. Furthermore, for an optimal performance and an extended lifecycle, belts and pulleys should be designed in such a way to obtain a high ratio between the pulley diameter and the belt thickness, since this parameters influence the bending stress the belt suffers every cycle as it goes around the pulleys, and is actually the most critical stress. Experimental results carried out by different belt manufacturing companies such as Belt Technologies Inc. and Sandvik, have shown that ratios (Diameter/thickness) of around 625:1 give the belt an expected life of over one million cycles, which is usually taken as a design reference for the following considerations.

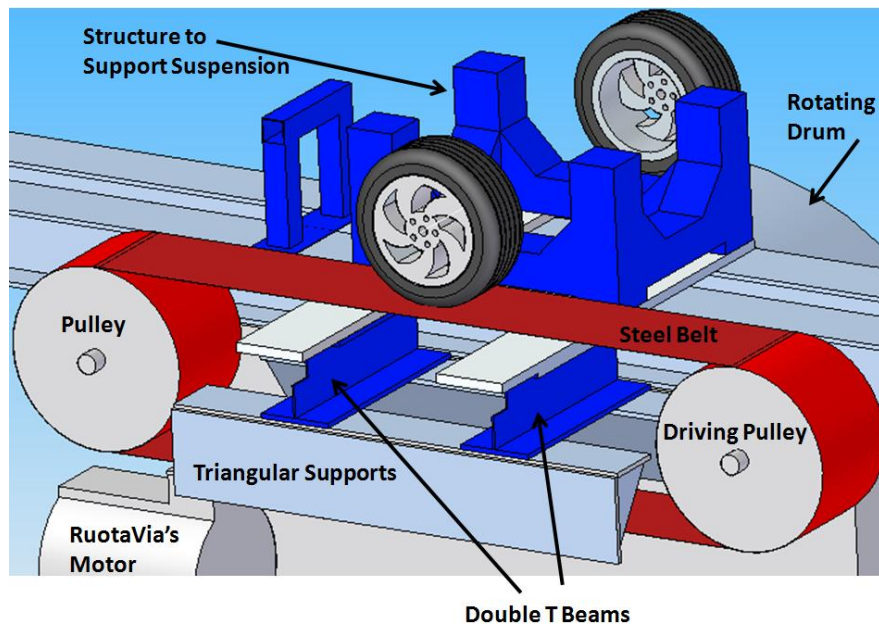


**Figure 12 - RuotaVia Stainless Steel Belt Rolling Road Scheme**

A 3D model of the RuotaVia Test Facility was created in order to assess the available space for the belt, pulleys and driving systems of the rolling road. The 3D model shows the double T section beams of the structure, the concrete wall at the center of the structure, the motor and the structure (in blue) used to support the suspension and the axle when an entire front or rear shaft is assembled in the rig. It can be seen how the double T beams of the RuotaVia limit considerably the available space to place the belt, as they cross just under the place where the second tire is. In order to achieve adequate sizes of the pulleys, it was necessary to make the belt rotate around the two beams (seen in blue).

The proposed stainless steel belt rolling road basic concept is also illustrated in the 3D model. One of the pulleys should be located over the RuotaVia's motor, which limits the available space for it. Instead, the second pulley has no other elements close to it, so the available space is more generous, and therefore was considered as the driving pulley, given the available space next to it for the driving motor and belt. The stainless steel belt is represented in red (we must remember usually a polymeric surface finish is used for this kind of applications). Given the space limitations identified with the 3D model, the dimensions for the belt and pulleys were determined. The main restriction for the pulley size was the location of the motor of the RuotaVia, while the triangular supports of the transversal double T beams made it mandatory to use a long distance between the centers of the pulleys (2.9 meters), and therefore a considerably long belt. Given the long distance between the pulley centers, it is possible to have belt sag at the un-tensioned side of the belt, for which might be necessary to use a stationary support to ensure the adequate tension of the belt. The sliding of the belt along this type of stationary surfaces in ultra-high molecular weight materials has been proved as having no effect on the belts performance.

Early in the design process, the huge size of the belt and pulleys was identified as a major limitation affecting the feasibility of this design, since the required dimensions would give low flexibility to the use of the rolling road, considering the belt would have to be welded at the test rig and around the beams. Therefore the possibility of implementing future changes to this design approach is very limited. However, the design was further developed, and with the available space it is possible to fit a belt with a 450 mm width, driven by 750 mm diameter pulleys. The space between the concrete walls is 932 mm, so with a 450 mm wide pulley, there would still be space available to fit the structure and the bearings required to support the rolling road and the driving system.

Belt Width	450 mm
Pulley Diameter	750 mm
Pulleys center distance	2900 mm

**Table 5 - Stainless Steel Belt Dimensions**

Once the main dimensions of the rolling road were determined, the design process was followed by the calculations of the torque and power requirements. The required motor torque must counteract the friction force between the belt and the supporting surface, considering the wheel rotates freely over the belt's surface. Therefore, the maximum required driving torque at the pulley may be

calculated as a relationship between the friction force experienced by the belt, and the radius of the driving pulley as follows:

$$F = \mu * N$$

$$T = F * r$$

Where  $\mu$  is the dynamic coefficient of friction (assumed as 0.04 as of the friction against a Teflon support) and  $r$  the radius of the driving pulley. Therefore, considering a normal force created by a mass of 1000 kg, as would be of a heavy vehicle, the required torque would be:

$$T = 0.04 * 1000 * 9.81 * 0.375 = 147.15 \text{ N} * \text{m}$$

The RuotaVia test facility has the capacity to achieve a maximum tangential speed of nearly 440 km/h (111.1 m/s), so the rolling road system for the opposite tire should be capable of achieving the same speed. The required tangential speed of the rolling road was set as equal to that of the rotating drum, since the steel belt can handle very high speeds, though later in the feasibility analysis it was lowered, since the system would hardly ever be used at those speeds. However, for analytical purposes, the calculations were done with the maximum speed, since lowering the speed would only alter the driving motor size. Therefore, the required motor power is calculated as:

$$P = T * \omega = T * \frac{v}{r} = 147.15 * \frac{111.1}{0.375} = 47.96 \text{ kW}$$

Once the required power and torque transmitted are known, it is possible calculate the working Load on Belt ( $F_w$ ) as described in the “Design Guide and Engineer’s Reference for Metal Belts” provided by Belt Technologies Europe.

$$F_w = F_1 - F_2 = \frac{T}{r} = 392.4 \text{ N}$$

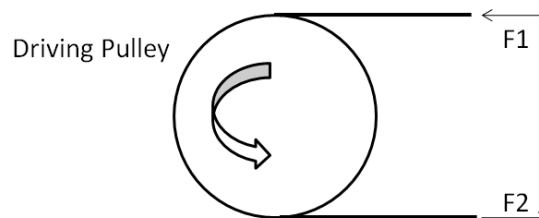


**Figure 13 - Driving Pulley Forces**

The force  $F_1$  is the highest acting on the belt, generated by the tension caused by the torque transmitted (by friction) from the driving pulley to the steel belt, while the force  $F_2$  is the tension at the opposite side of the belt. For friction drive systems, like the one here considered, where the belt is driven only by the friction between itself and the pulley, the non-slip condition of the belt on the pulley is obtained when the following condition is satisfied:

$$\frac{F_1 - F_c}{F_2 - F_c} = e^{\mu\theta}$$

In the former equation,  $\mu$  represents the static friction coefficient between the belt and the pulley,  $\theta$  is the angle (in radians) along which the belt is in contact with the pulley known as wrap angle (which corresponds to 180 degrees for a 2 pulley system), and  $F_c$  is the inertial force caused by the belt's rotation around the pulley. However, the inertial term is usually neglected for metal belts, which have a very low mass since their thickness is in the order of fractions of millimeters, in this case 0.8 mm. For this particular belt system with only two pulleys, the contact angle is obviously equal to  $\pi$  radians, and the friction coefficient is around 0.35 (calculated as the friction between a machined metal pulley with a stainless steel belt). Manipulating the two former equations, and neglecting the inertial term, the required tension on the belt is:

$$F_1 = \frac{e^{\mu\theta} F_w}{e^{\mu\theta} - 1} = 588.3 \text{ N}$$

The tension is an important aspect to control in belt systems, since low values lead to slip between the pulley and the belt, while high values usually affect the life of the belt and generate an increase in the wear of other components as the bearings. Therefore, it is desirable to operate the belt under the lowest possible tension, for which the design of a mechanism to change and control the tension of the belt is required such as springs or screws acting in one of the shafts. Once the required forces on the belt have been calculated, it is possible to calculate the stresses acting on the metallic belt, which are basically two.

The most relevant stress on the belt is the bending stress ( $\sigma_b$ ) caused by the cyclic flexion while rotating around the pulleys. The bending stress increases as the diameter of the pulleys decreases, and it is the reason why big pulleys are desired to improve the lifecycle of the belt. The second stress component acting in the belt is caused by the tension required for the non-slip condition between belt and pulley, which causes a stress known as working stress ( $\sigma_w$ ). The total stress ( $\sigma_T$ ) acting on the belt is given by the sum of the two stresses. The calculation of the stresses in terms of the diameter of the pulleys  $D$ , the belt

thickness  $t$  (chosen from those available in a catalogue as 0.8 mm), the belt width  $b$  and the Poisson modulus  $\nu$ , are done as:

$$\sigma_b = \frac{E * t}{(1 - \nu^2)D} = \frac{202000 * 0.0008}{(1 - 0.285^2)0.75} = 234.5 \text{ MPa}$$

$$\sigma_w = \frac{F_1}{b * t} = 1.6 \text{ MPa}$$

$$\sigma_T = \sigma_b + \sigma_w = 236.15 \text{ MPa}$$

Recognized metal belt producers such as *BELT TECHNOLOGIES* recommend that the total stress on the belt should not exceed one third of the material's yield strength, in order to avoid reducing drastically the expected life of the belt, which as previously mentioned basically depends on the diameter/thickness ratio. Considering this, the calculated value of the total stress is adequate, since the yield strengths of the stainless steels used for these belt applications (such as the 301 or 304 full hard alloys) are over 1100 MPa, which gives some safety margin over the rule of thumb.

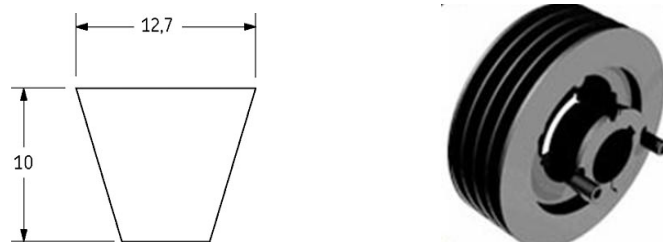


**Figure 14 – Power Transmission for Steel Belt. Belt Section and Pulley**

Due to the space limitations at the RuotaVia test facility, the most adequate power transmission system to drive the pulley was a rubber belt. Belts are an easy way to transmit power and offer many advantages such as low noise and are good enough to transmit high power as required in this case. Remembering that the estimated required power is nearly 48 kW (64.3 hp) in order to drive the belt and load to the top speed of 440 km/h, a rotational speed of 3112 rpm is required at the driving pulley of the rolling road. Given the power transmission parameters, the required belts and pulleys were selected based on the Power Transmissions Calculations from SKF. For a rated power of 48 kW and a DC motor running at 1750 rpm, a possible solution based on the SKF power transmission catalogue would be given by a 180 mm diameter driver pulley (PHP 6SPA180TB) and a 100 mm driven pulley (PHP 6SPA100TB), driven by 6 belts of the type PHG XPA2000 from the SKF catalogue.

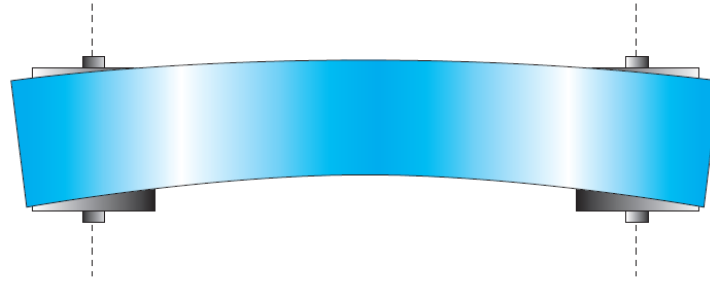


**Figure 15 - Belt Tracking Defect**

The construction of steel belts requires the construction of a stiff structure to support the belt, while also having a relatively simple assembly method (due to the space limitations) and offering a way to tension the belt. An insufficiently stiff structure will bend when the belt is tensioned and will therefore generate a difficulty to control the motion, since the system will be deformed. An additional problem present in the construction of metal belts is known as belt tracking. Since metal belts cannot stretch as a rubber belt would do, it is not able to compensate for deflections of the shaft, or lack of alignment and the single belt cannot withstand increasing lateral forces. In example, if the belt was not precisely welded, the circumference of one border will be slightly different from the other one, and so one edge will be exposed to higher stresses than the other one. Therefore, a belt tracking technique must be considered to correct the problem and keep the belt in its central position over the pulleys. Among the possible solutions, the *Pulley Axis Adjustment* is widely used, consisting in slightly changing the angle of the shafts (ideally one, but in practice just one is good enough) to compensate the defect and control the tension. In more complicated cases, the compensation may be done by *Forced Tracking*, by attaching a V rubber belt to the internal side of the metal belt, and making a groove the pulleys.

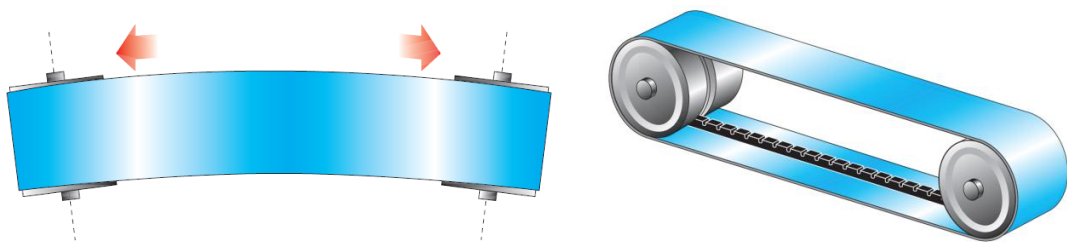


**Figure 16 - Pulley Axis Adjustment and Forced Tracking**

Even though a stainless steel belt is the state of the art solution for a high performance rolling road designs, and it could adequately perform at the

RuotaVia, early in the design process it became evident that this solution's performance exceeded the real requirements that could arise during testing. When testing suspension system it is usually done at moderate speeds and therefore the rolling road will probably never be exposed to such high speeds as the ones previously considered as design parameters. In fact, suspensions are usually tested at relatively low speed (up to 100 km/h), while high speeds are used to specifically test tires. Besides, building a rolling road able to match the maximum performance of the RuotaVia test rig requires a very big and complex system difficult to setup in the reduced available space and would therefore have low operation flexibility, since modifying or removing the system would be a hard task. Therefore the implementation of such a system would not be justified given the use it would actually have. Even considering the economical point of view, the project became unfeasible, since just the price of such a big motor (nearly 50 kW) was excessive, considering such high speeds would never be truly required and therefore that amount of power is not necessary.

Besides the excessive performance parameters previously considered, other difficulties were found with the metal belt design characteristics which lead to the decision of dropping down the idea. Since the metal belt of the rolling road rotates around the structural beams of the RuotaVia (which are fixed and cannot be moved), the belt would have to be welded in the sight. Welding the belt in the sight meant that the belt could not be easily removed if necessary, and even more, the tolerances of the welding could not be guaranteed when welding having to weld at the test rig, which would lead to tracking problems. Therefore, a metal belt solution for the rolling road was not flexible in its operation, and requiring such accurate welding on the site would increase the costs. Finally, the huge size of the overall system meant that a complex supporting structure would be required to support the pulleys and give the belt and adequate tension, which given the space limitation was a unnecessary design challenge to built an unpractical system. As a result of the former considerations a new approach was taken for the design of the rolling road, based on a rubber belt which will be further developed ahead in this document. Though a rubber belt rolling road is definitely not a state of the art solution for a rolling road, it emerged as a feasible option for the testing at the RuotaVia test Rig, since a compact rolling road could be built, fitting adequately in the available space, and offering more flexibility in its operation, even making possible to remove it or displace is if necessary. Rubber belts have a much lower speed limit, are more vulnerable to wear effects, and of course have a lower strength to weigh ratio compared to steel belts. Though using a rubber belt made friction a bigger concern in the design process, it became an interesting option for this project.



### 3.3 Rolling Road Design with Poly-V Belt

Considering the space limitations at the RuotaVia test facility, and given the complexity and difficulties found while working on a steel belt design, a simpler design was approached, based on a rubber Poly-V belt supported pneumatically with and externally pressurized air bearing. For the new design approach, the calculations were done based in the actual test parameters usually used in testing applications like suspension vibration analysis were the rolling road would be used. In the new design approach not only in the implementation of a rubber belt rolling road was considered, but also changing the maximum rotation speed that the belt should reach by reducing it from 440 to 100 km/h. The considerable speed reduction meant a much smaller motor and belt transmission systems are required, which considering the space limitations is a great advantage also in the economic aspect.

Once again, vertical force of nearly 10000 Newton was considered as the load transferred by the tire to the belt. Analog to the case of the stainless steel belt, the power losses in the system are due to the friction between the belt and the supporting surface. Unlike the flat cross section of steel belts, rubber belts have different sections such as the poly-V belts which have ribs that enhance the performance of the belt by increasing the area in contact with the pulleys. Given the shape of the cross section, and the much higher friction forces that occur between rubber and other materials, this approach required a more elaborated approach to the supporting surface under the belt. This necessity lead to consider the possibility of designing an externally pressurized air bearing pad to give pneumatic support to the rubber belt while reducing considerably the friction.

Basically, the air bearing is an aluminum box fed with compressed air, and having the grooves to guide the belt's ribs along one of its faces. Along the ribbed face many small orifices are homogeneously distributed along the surface, through which compressed air is ejected at high speed against the belt, creating an air film between the belt and the bearing. The air film gives support to the belt and its load while reducing the resistance of the belt to move caused by friction, as the surfaces are not anymore in direct contact. However, due to the ribbed surface of the belt, the design of the air bearing was a challenge, since nothing of similar characteristics has been done.

Theoretically, air bearings may reduce friction between components to zero. However, such a high efficiency for an air bearing is tightly linked to strict tolerances in the air gap between the parts of interest, which in modern state of the art bearings is in the order of microns. Considering the possible losses that

might arise, a resistant force  $F_r$  due to friction equivalent to 2% of the vertical load was assumed for the design calculations.

$$F_r = F_z * 0.02 = 200 \text{ N}$$

Given the resistant force, it is now possible to calculate the resistant power, lost due to friction, which the motor must provide, to drive the belt up to a speed of 100 km/h.

$$P_r = P_r * v = 200 * \frac{100 \text{ km/h}}{3.6} = 5.55 \text{ kW}$$

### 3.4 Selection of the Poly-V Belt

The selection of the rubber belt to use was based in the belts and pulleys available in the catalogue of the company *Poggi Trasmissioni Meccaniche*. Poly-V belts have longitudinal ribs in V shape, which run along the pulleys, which must have grooves with the shape of the ribs to guide the belt. The shape of the ribs increases the contact area between the belt and the pulleys, improving the power transmission. In the case of Poly-V belts, the contact area is 3 times higher than that one in a flat belt with the same dimensions and so the slip between belt and pulley is reduced.

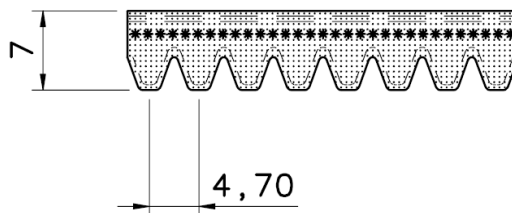


Figure 17 - POLY-V belt L type section

A POLY-V rubber belt is described by three main characteristics, the cross section, the number of ribs and the total length. Three main cross section types are available, denominated as J, L and M, for which the height and pitch varies. The pitch and the height increase passing from J to L and finally M section profiles. Concerning the length of the belt, it is measured at the bottom of the ribs, which when assembled correspond to the outside diameter of the pulleys. The rolling road requires a relatively small belt since it should fit in the space available between the two double T beams (600 mm), and also an adequate belt

height to prevent the belt from moving to the sides when subjected to lateral forces by the tire. The smallest M profile belt is around 2300 mm long, and therefore was immediately ruled out. Therefore, the selection was done between the J and L profile belts, which have pitches of 2.34 and 4.7 mm, and heights of 3.5 and 7 mm respectively.

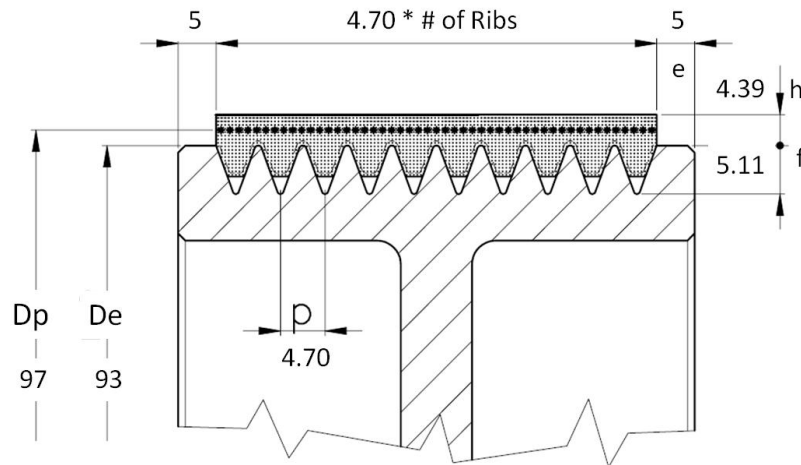


Figure 18 – L Section Belt and Pulley Dimensions

The selected rolling road POLY-V belt was the L section, which is considerably higher than the J profile (though the J profile had a higher speed limit of 60 m/s), and would therefore perform better when subjected to lateral forces. The L belt profile has a pitch (distance between ribs) of 4.7 mm, which multiplied by the 72 ribs, provides a rolling road width of 338.4 mm. L section belts have a speed limit of 50 m/s according to the manufacturer's catalogue, so it is adequate for the rolling road, which should normally not exceed 100km/h (27.7 m/s). Among the available L section belts, different possibilities were studied between the belts with the smallest lengths (those ranging from 954 to 1075 mm), in order to design a compact rolling road.

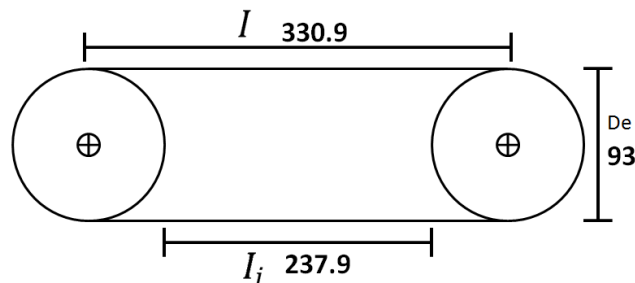
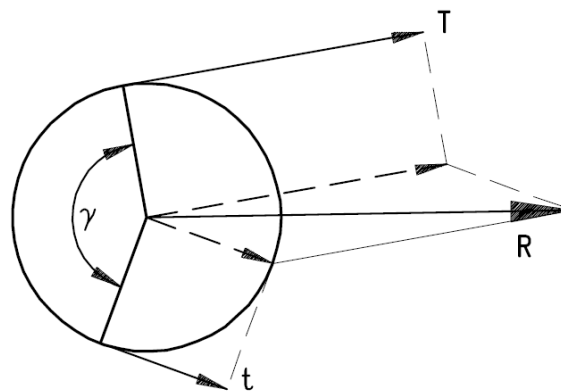


Figure 19 - Rolling Road Basic Dimensions

Among the smallest available belts a 954 mm long belt (code 11L0954) was found (with a corresponding tolerance of +5 and -10 mm) for which was available a 93mm diameter standard size pulley which was selected to drive the rolling road's rubber belt. With the belt and pulleys dimensions known, it then was possible to calculate the required distance between the pulley shafts, and the available space between the belt and the pulleys to fit the supporting air bearing.

$$I = \frac{L - \pi * D_e}{2} = 330.9 \text{ mm}$$

$$I_i = I - D_e = 237.9 \text{ mm}$$



**Figure 20 - Resultant force on Pulleys**

The dynamic stresses on the belt due to the tension and the rotation create a resultant force  $R$  that acts on the pulleys. The magnitude and direction of the resultant force depends of the wrap angle of the belt around the pulley, the friction coefficient between the belt and pulley (which is 0.435 for aluminum pulleys according to the literature), and the speed of the belt. According to the catalogue ([3] page 64) of this type of POLY-V belts, for the case of the belt running at 100 km/h (27.77 m/s) with a wrap angle  $\gamma$  of 180 degrees, the resultant force is 3.6 daN per kW. Therefore, for the previously calculated power of 5.55kW, a total resultant force of 200 N is generated, which is a load that must be supported by the bearings. It is important to notice that according to the information in the catalogue, the resultant force  $R$  (per kW) decreases as the speed of the belt increases (for a given wrap angle) probably as a result of the increasing inertial forces acting on the belt as the speed increases. For the particular case of a wrap angle of 180 degrees, obviously the resultant force is acting in the horizontal direction.

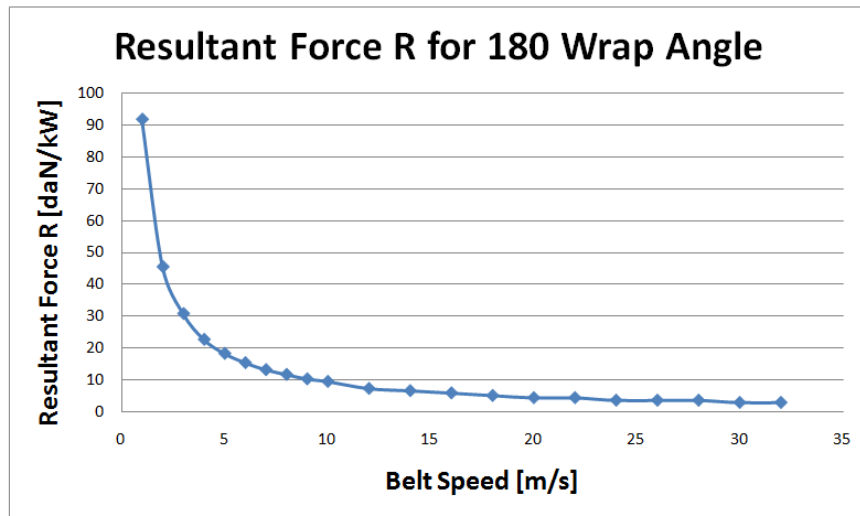


Figure 21 - Resultant Force on Pulleys

The required rotational speed of the rolling road pulleys can be calculated according to the required speed of the belt  $v$ , at which the tires need to be driven during the tests, which was set as 100 km/h. Given the external diameter of the pulleys  $D_e$ , and the belt height  $h$ , the angular speed of the pulleys can be calculated as:

$$w_{pulley} = \frac{v}{\left(\frac{D_e + 2h}{2}\right)} = 545.8 \frac{rad}{s} = 5211.4 \text{ rpm}$$

Given the high speed at which the belt is rotating around the pulleys, the inertial forces must be considered and calculated since the inertia causes an additional tension in the belt, which must be added to the resultant force generated by the belt's tension. We must remember in the case of metal belts, effects due to inertia were neglected, since the unit length weight of the metal belts is quite small, but in the case of rubber belts is not negligible. The centrifugal stress on the belt (considering the 72 ribs, and a 100kph speed) is given by:

$$F_c = 2 f_c \sin\left(\frac{\gamma}{2}\right) = 4824 \text{ N}$$

In the former expression the term  $f_c$  represents the overtensioning in one of the sides of the belt caused by the centrifugal forces acting in it. The values of  $f_c$  are provided by the manufacturer as a function of the belt's linear speed and the number of ribs it has. For the rolling road's the overtensioning is equal to 335 N

for each 10 ribs. And therefore the total resultant force acting on the pulleys is given by:

$$R_o = R + F_c = 200 + 4824 = 5024 \text{ N}$$

The assembly of the belt must be done by marking too points at a known distance from each other and then tensioning the belt until the distance between the points increases by 0.5%. This assembly procedure requires a pulley center distance assembly range of around 20 mm for a belt of less than 1 meter length like the one considered for the design, so it this aspect was considered for the design of the supporting structure.

The belt itself is not capable of supporting the loads imposed by the wheel rotating over it. As a consequence, it was necessary to design a way to support the belt from bellow so that the load of the tire would not be supported by the belt and the pulleys. Any direct contact supporting method would generate a friction force between the belt and the support as the belt slides over the support. This friction dissipates the power that the driving motor must provide to the belt so it must be reduced to improve the rolling roads performance and controllability. Since the friction is directly proportional to the driving torque required, the bigger this force is the bigger will be the motor required to drive the system.

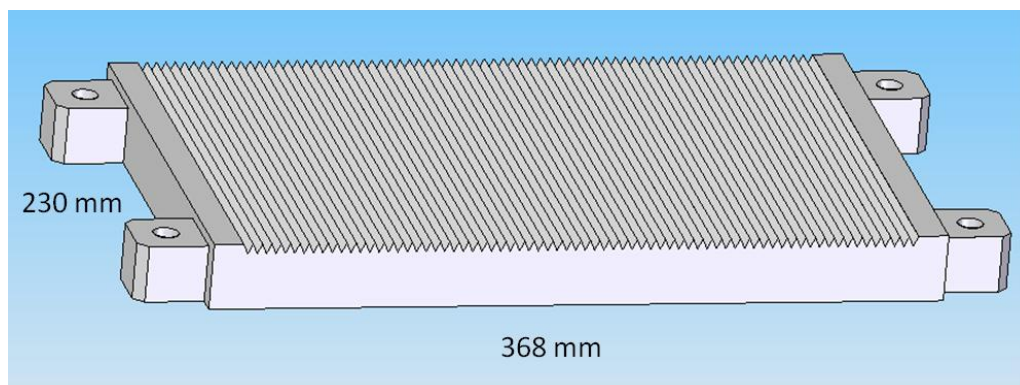


**Figure 22 - Air Bearing Support for Rolling Road Belt**

The best solution for the friction problematic was supporting the belt pneumatically, with a pressurized air cushion, created with an air bearing. Externally pressurized air bearings are elements that can reduce friction between moving elements by creating a small fluid film between them. Such elements may theoretically reduce friction between elements to zero, since no direct contact is present, and the pressurized air makes the parts literally float one relative to the other. Considering the high friction forces that would arise from

the rubber belt sliding over any surface, making it float over the supporting surface became an interesting alternative. Given the available space between the belt and its pulleys, the bearing was designed as a kind of grill, having on its surface the grooves to guide the ribbed belt as shown in figure 22. The pneumatic support is provided by pressurized air exiting orifices along the grooved surface that provide a vertical force that supports the load over the belt. Further ahead in this document a more detailed explanation about air bearings, their characteristics and design will be offered.

### 3.5 Transmission System

The design of the transmission system to drive the rolling road was also based on a POLY-V belt driven by an electric motor. Once again, the system was designed based on the catalogue of the company *Poggi Trasmissioni Meccaniche*.

Driving belts are selected based on the design power  $P_c$ , which corresponds to the required power to drive the system, multiplied by a correction factor. The correction factor  $C_c$  is useful to take into consideration different factor of the power transmission such as the starting torque, the type of machine to drive, and the service conditions, which are not taken into account in the power requirements calculated for steady state conditions. Correction factors are in the range between 1 and 2, according to the type of loads, and working conditions. Given the peculiarity of the application of belts in the rolling road system, it was quite difficult to determine in which classification group the application would best fit. Given the required high speeds and loads the belt should support, the working conditions could be compared to those of a heavy duty conveyor, with a moderate number of working hours each day. Therefore, according to the parameters given in the catalogue (pages 47 to 50 of [3]) for motor classifications, the type of driven machine and the working cycles, a correction factor of 1.5 was chosen, and the design power was calculated.

$$P_c = P_r * C_c = P_r * 1.5 = 8.33 \text{ kW}$$

According to the rpm of the smaller pulley and the design power, the type of belt section that best fits the application is suggested by the design catalogue. For a design power of 8.3 kW and a rotating speed of 5211 rpm, either section types J and L appear to be adequate, and so they were both analyzed. At this point it is important to check the maximum speed of the belt, since each section type has an operating limit, in this case 60 m/s for J section belts and 50 for the

L ones. The speed of the driving belt can be calculated based on the driven pulley of the rolling road, and so we notice both types of belts are adequate.

$$v_{belt} = w_{pulley} \frac{D_e}{2} = 545.8 \frac{0.093}{2} = 25.38 \text{ m/s}$$

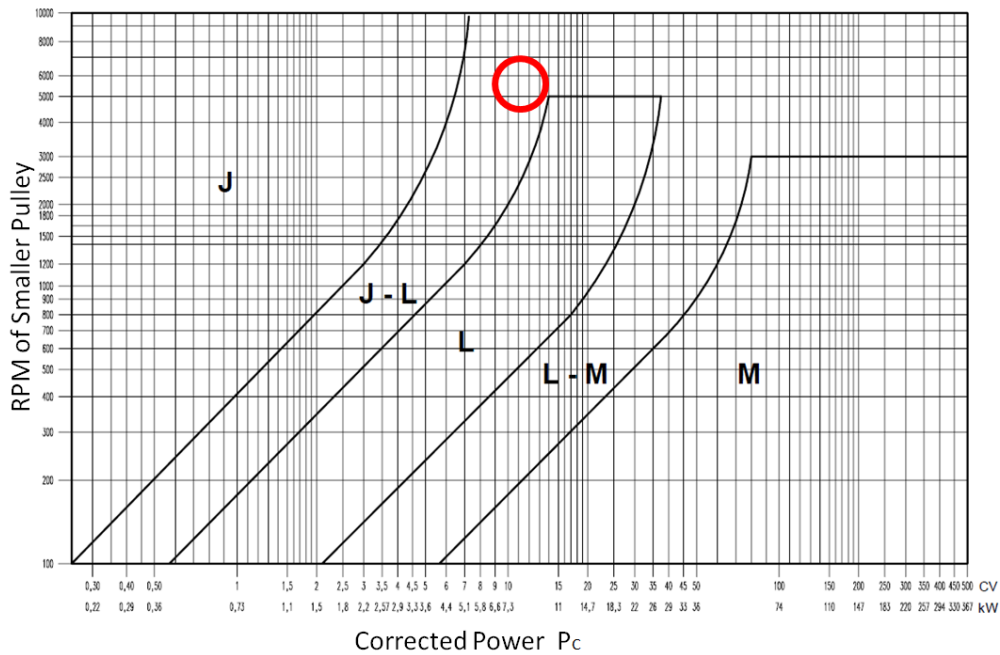


**Figure 23 - Belt Selection for a given Power and RPM.**

A typical electric motor like the one to be used for driving the system operates at a speed of 3000 rpm. Since the required rotation speed of the pulley at rolling road is known, it is possible to determine the required transmission ratio  $\tau$  that must be used between the motor and the rolling road to achieve the desired speed top speed of 100 km/h at the rolling road belt.

$$\tau = \frac{w_{pulley}}{w_{motor}} = \frac{5211 \text{ rpm}}{3000 \text{ rpm}} = 1.74$$

Once the transmission ratio has been calculated, it is possible to calculate the dimensions of the required pulley at the motor, remembering that the second pulley of the transmission has the same size as the pulleys of the rolling road. With the dimensions of the pulleys it is then possible to calculate the length of the transmission belt, based on the theoretical center distance between the pulleys ( $I$ ), and the external diameters of the transmission system pulleys. Given the



dimensions of the overall system, a center distance of 270 mm was estimated for the transmission pulleys. For a given power and rpm, a minimum diameter for the small pulley is given, which allows the design of a compact transmission, which for the case of 8 kW and 5200 rpm is between 60 and 67 mm. However, given the previously selected dimensions of the pulleys for the rolling road, one of which is part of the transmission, the same minimum value of 93 mm was assumed for the transmission, from which was also possible to calculate the required diameter for the motor's pulley  $D'_e$ . Though using larger pulleys than the minimum suggested ones for the given power and rpm gives as a result a bigger size transmission, it has been proved that the life of the belt is considerably extended when slightly increasing the pulleys diameter.

$$d_e = 93 \text{ mm}$$

$$D'_e = d_e * \tau = 161.8 \text{ mm}$$

The diameter for the motor pulley given by the exact transmission ratio is not available among the standard pulleys available, and therefore the closest pulley available for the given type of belt section was chosen. For the L type section belt, the closes diameter to 161.8 mm corresponds to a 153 mm pulley (code 12L16008) while for type J belt it corresponds to 158 mm (code 12J16008) as seen on pages 8 and 12 of the catalogue. Once chosen the diameters of the pulleys and the nominal center distance  $I_t$ , is possible to calculate the theoretical length of the transmission belt  $L_t$ .

$$L_t = 2 * I_t + 1.57(D'_e + d_e) + \frac{(D'_e + d_e)^2}{4 * I_t}$$

With the theoretical length of the belt known, it is the necessary to compare this value with the actually available standard belt lengths  $L_e$ , and select the belt with the most similar characteristics to those previously calculated. By calculating the difference between the theoretical length and the available ones and minimizing it, the 955 mm long J section belt and the 954 mm L section belt were the most adequate. Once the belts are chosen, it is possible to calculate the actual center distance between the pulleys.

$$I_e = I_t + \frac{L_t - L_e}{2 \sin\left(\frac{\gamma}{2}\right)}$$

In order to calculate the actual distance between centers, it is also necessary to know the warp angle. The wrap angle  $\gamma$  is an important factor to calculate when

designing belt transmissions where the transmission ratio is considerably different from one. The wrap angle indicated the contact angle between the pulley and the belt, which obviously affect the adherence and friction conditions between the belt and pulley, and as a consequence the efficiency of how the power is being transmitted. The wrap angle is always referred to the smallest diameter pulley since it is the one working in the most critical condition in a 2 pulley system and therefore, the wrap angle is at most equal to 180 degrees, in the case where both pulleys have the same dimensions. Otherwise, the wrap angle (in degrees) can be calculated as:

$$\gamma = 180^\circ - 57 \frac{D'_e + d_e}{I_e}$$

By solving simultaneously the equations of the wrap angle  $\gamma$  and the center distance  $I_e$ , it is possible to obtain the actual center distance required for the J and L section belts. A final important consideration when designing a belt transmission system is known as power rating calculation. The power rating is the actual power that the belt and pulleys actually transmit and are therefore available according to the losses that might arise. The basic performance ( $P_b$ ) values given by the manufacturer refer to the amount of kW that a single rib can offer. However, the given values for each type of belt were experimentally determined for very particular conditions such as a transmission ratio of 1, wrap angles of 180 degrees and for particular ranges of belt lengths. Therefore, an adjustment process must be done in order to determine the actual available power according to the particular parameters of each transmission.

$$P_t = (P_b + Cr) * C_\gamma * C_I \quad [kW]$$

The power adjustment is done by means of a series of coefficients to obtain the actual available power that the transmission offers according to the different parameters such as belt type, pulley diameters and operation speed. The  $Cr$  coefficient corrects the power rating according to the transmission ratio  $\tau$ . The second factor is  $C_\gamma$ , which corrects the power depending on the wrap angle, as it varies in the range between 230 and 100 degrees. The last factor is  $C_I$  and it corrects the power according to the belt type and length. With these three coefficients and the basic performance power is possible to determine the actual power that will be available to drive the rolling road.

Once the power rating  $P_t$  was been calculated, it was possible to determine the minimum number of ribs  $Q$  required in the belt to transmit the power to the rolling road. For the J section belt, at least 5 ribs are necessary, while for the L section only 3 would be enough. The final analysis lead to the selection of an L

section belt, (954 mm long with 8 ribs) which is more than enough to transmit the power, and the pulley is just 46 mm wide. The selection of this belt was an interesting option since it is the same type of belt used for the rolling road.

$$Q = \frac{P_c}{P_t}$$

The following table resumes the power adjustment calculations and the values of each coefficient for both the J and the L section belts that were considered.

	Type Of Belt Section	
	J	L
<b>P<sub>b</sub> [kW/rib]</b>	1.652	3.589
<b>γ [degrees]</b>	167.59	168.54
<b>Cr: Ratio correction coefficient</b>	0.05	0.57
<b>C<sub>γ</sub>: Wrap angle correction factor</b>	0.97	0.97
<b>Cl: Belt length correction factor</b>	1	0.9
<b>P<sub>t</sub> [kW/rib]</b>	1.65	3.63
<b>Required Number of Ribs</b>	5.05	2.29
<b>L<sub>e</sub>: Belt Length [mm]</b>	955	954
<b>Belt Width [mm]</b>	14.04	14.1
<b>D'e: Motor Pulley Diameter [mm]</b>	158	153
<b>Pulley Width [mm]</b>	45	46
<b>l<sub>e</sub>: Center Distance [mm]</b>	300	300

Table 6 - Transmission Belts Main Parameters

With the center distance between pulleys (30 cm) and the diameters of the transmission system pulleys it is possible to calculate the wrap angle of the transmission belt around the smaller pulley  $\theta$ , and the angle  $\alpha$ , indicating the direction of the belt's tension relative to the pulley.

$$\alpha = \tan^{-1} \left[ \frac{D_e - d_e}{2l_e} \right] = 5.7^\circ$$

$$\theta = \pi - 2\alpha = 168.6^\circ = \gamma$$

The final design calculations concern the forces, moments and stresses at the shafts of the rolling road pulleys due to the transmitted power and the belts tension. The required torque at the driving pulley M of the rolling road can be calculated based of the pulley's diameter and the resistance force on the belt due

to friction (as calculated for the steel belt case in section 3.2) and considering the effect of the higher torque required when starting the system.

$$M = \left[ F_r * \frac{de}{2} \right] * 5 = 46.5 [N * mm]$$

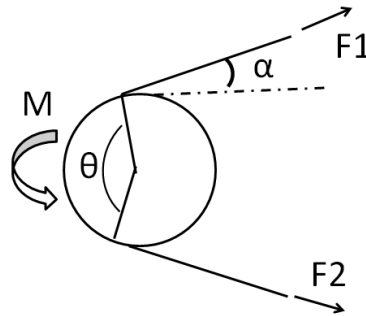


**Figure 24 - Angles of Belt and Pulley**

Once the driving torque of the rolling road is known, it is possible calculate the forces that that the belt's tension produces in the pulleys shaft. The difference between the forces  $F_1$  and  $F_2$  is associated with the driving torque  $M$  and pulleys diameter. We can then calculate the required initial tension (as in [16] pg. 873) in the belt as:

$$F_i = \frac{e^{\mu\theta} + 1}{e^{\mu\theta} - 1} * \frac{M}{de} = 706.5 [N]$$

Then, by considering the additional tension due to the inertial of the belt, the forces  $F_1$  and  $F_2$  can be calculated as:

$$F_1 = F_c + F_i \frac{2e^{\mu\theta}}{e^{\mu\theta} + 1} = 1474 N$$

$$F_2 = F_c + F_i \frac{2}{e^{\mu\theta} + 1} = 474 N$$

By separating the horizontal and vertical components of  $F_1$  and  $F_2$  and adding them, we obtain the total load generated by the belt of the shafts.

$$T_0 = (F_1 + F_2) \cos \alpha = 1939 N$$

$$T_{vertical} = (F_1 - F_2) \sin \alpha = 99.5 N$$

$$T_{total} = \sqrt{T_0^2 + T_{vertical}^2} = 1941 \text{ N}$$

$$M_f = T_{total} * 83 = 161103 \text{ N} * \text{mm}$$

Now that the tension of the rolling road's belt and the transmission belt have been calculated, it is possible to calculate the total load in the main shaft of the rolling road. This shaft must support not only the tension of the rolling roads belt, but also the extra load generated by the transmission belt, which being at the outside of the shaft creates a bending moment. By adding the components of the tension of the rolling road's belt and the tension  $R_o$  components of the driving belt  $F_1$  and  $F_2$ , we obtain a total horizontal force of 5697 N, and a vertical force of 1819.8 N and therefore, the total load  $R_{total}$  is equal to 5980 N at an angle of approximately 18 degrees. Evidently, these loads must be considered for the selection of the bearing that supports the rolling road's shafts.

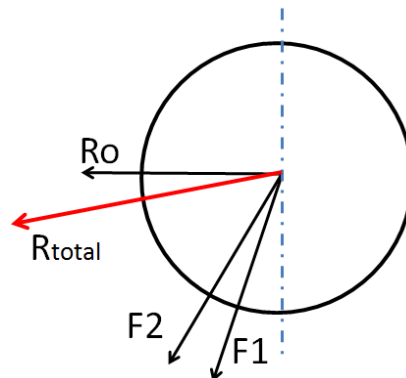


**Figure 25- Loads at the Rolling Roads Main Shaft**

Once the forces acting on the shaft are known, the bending stress on the shaft caused by the load in the external driving pulley must be assessed, since it will be the most important stress present in the system. A 35 mm diameter shaft was chosen in order to easily fit the standard pulley dimensions, and considering a low bending stress is required to guarantee the adequate performance of the shaft for a long lifecycle. The distance between the bearing's center and the driving pulley is 83 mm, with which the bending moment at the shaft caused by the forces at the pulley can be calculated as:

$$\sigma = \frac{32 M_f}{\pi D^3} = 38.27 \text{ [MPa]}$$

## 3.6 Rolling Road Structure

Once all the main elements of the rolling road system such as belts and pulleys were selected, a structure was designed, in order to support the different elements such as the roller bearings and their housings, the pulleys and the air bearing. An important aspect of the supporting structure was that it should allow some displacement range between the center distance of the pulleys, not only of the rolling road but also the ones of the transmission, in order to assemble the rubber belts around the pulleys and tension them.



**Figure 26 - Rolling Road Render**

The entire rolling road system (except the motor) is supported over 4 double T shaped beams, two of which are already welded to the structure and were previously used for supporting the wheel. These beams are 600 mm long and therefore fit exactly in the available space between the RuotaVia's structural beams. Over the beams, rests a 560 x 536 mm aluminum plate (18 mm thick) which is fixed to the four beams by 16 M10 bolts distributed along both sides of the structure. The pulley holding the driving pulley remains fixed, and therefore the tensioning of the rolling road's belt is done by displacing the shaft of the second pulley. The motion of the pulley is achieved thanks to a moving plate, which supports the second pulley, and can be fixed in the desired position by means of slotted holes, which give the moving plate the option of extending the center distance up to 20 mm in the direction perpendicular to the pulleys axis, which is between the margin suggested by the manufacturer to assemble and

tension this type of belt. The center distance (and therefore the tension) of the belt is controlled by adjusting two screws (one at each side of the belt), which are fixed to the main plate, and can push the tensioning plate and hold it is fixed in the desired position. On the other hand, the tension of the transmission belt is controlled by displacing the motor, which is supported over a movable plate which allows the motor to move up to 90 mm in the horizontal direction.

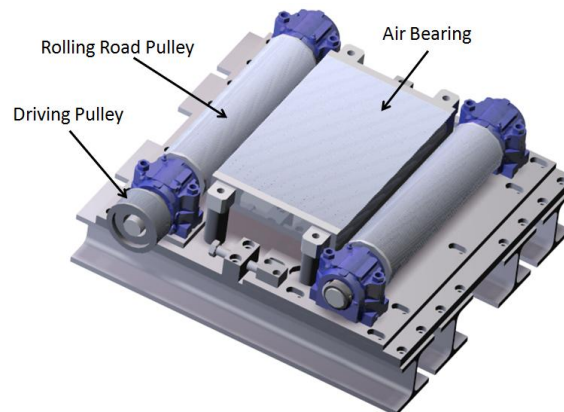


**Figure 27 - Rolling Road without the Main Belt**

The air bearing is supported between the span of the belt by four fixed aluminum cylinders, through which the four M12 bolts that support the air bearing pass. Since the air bearing remains fixed even when the belt is being tensioned, two of the cylindrical supports pass through slotted holes in the tensioning plate. Finally, two additional supporting plates were required to adjust the height of the main pulley due to the additional height of the second pulley due to the tensioning plate.

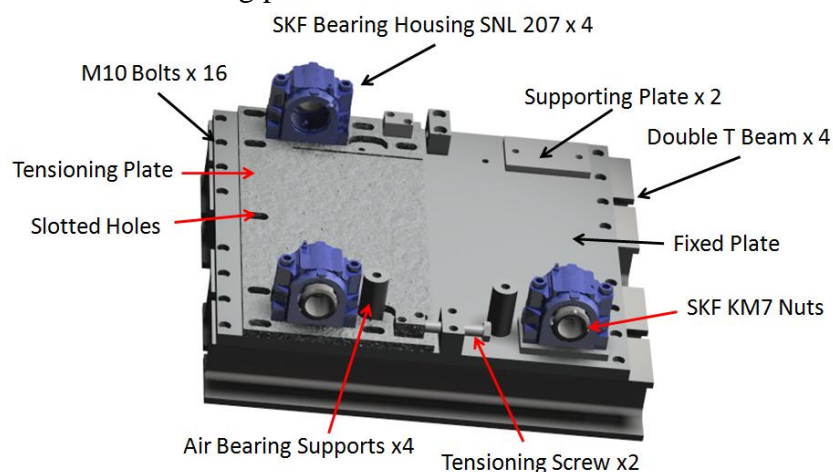


**Figure 28 - Rolling Road Structure Main Components**

The pulleys are supported by four single row angular contact bearings (SKF 7207) which have a 35 mm diameter. This particular bearing is rated to work with a dynamic load of 31 kN and a speed of 12000 rpm and is therefore more than adequate for the rolling road application. Angular contact bearings have the inner and outside rings contact points slightly displaced in the direction of the bearing's axis. The displaced contact points allow this type of bearing to support simultaneously combined loads in the axial and radial directions.

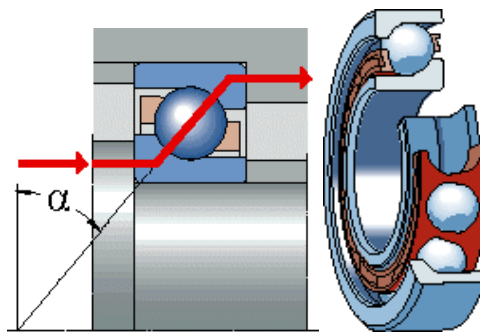


Figure 29 - Angular Contact Bearings

The capability of angular contact bearings to support axial loads increases as the contact points in the inner and outer rings are further displaced, which increases the contact angle  $\alpha$  (the angle between the line connecting the contact points and a vertical line, in this case 40 degrees). The angular contact is achieved by introducing high shoulders in the bearing rings. However, single row angular contact bearing can only accommodate axial loads in one direction, and therefore they are usually used in pairs, as in the rolling road case, where the bearings were mounted in a Back-to-Back configuration in each shaft, which gives the system a bidirectional load support capability, which is important considering the belt will be loaded by the tire not only vertically, but also eventually laterally.

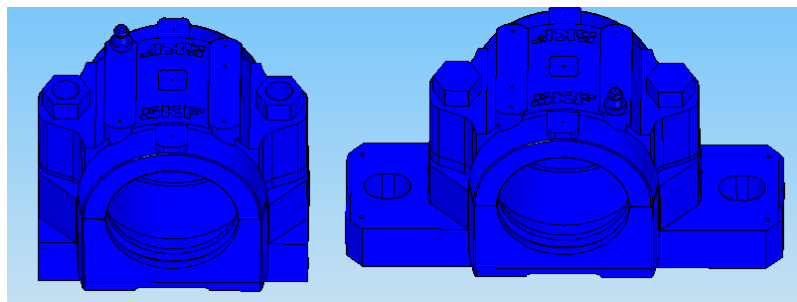
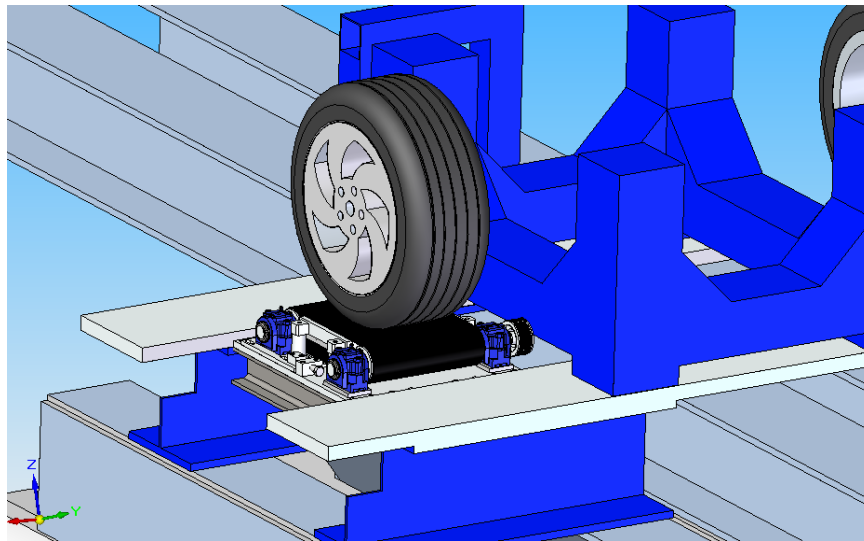


Figure 30 - SKF Bearing Housing Modification

Each roller bearings is fixed to the rest of the structure by an SKF bearing housing (of the type SNL 207). In order to be able to fit these housings in the



rolling road's structure, it was necessary to make them a slight modification to reduce their size. The standard housings have use four bolts, two of them to close the housing after fitting the roller bearings inside, and two additional bolts to fasten the housing to the external structure. The standard housings were 185 mm long, since the fastening bolts are placed at the sides of the housing. In order to make them fit in the structure, the sides of the housings were cut and removed, and the bolts previously used to close the housing were further drilled to the bottom, and therefore used also to fix the housing to the structure, making the modified housings just 114 mm long. Finally, the shafts of the pulleys were constrained in the axial direction by lock nuts (type KM7 from the SKF catalogue) which may carry axial loads of up to 50 kN



**Figure 31 - Rubber Belt Rolling Road in the RuotaVia Test Rig**

Figure 31 shows the concept of the POLY-V rubber belt rolling road set at the RuotaVia test rig, supported between the transversal double T beams (in blue). As seen, the proposed design is quite compact (if compared to the size of an average size vehicle tire), and is therefore easily removed if necessary by just removing some bolts. Therefore, compared to the previously studied stainless steel belt rolling road, this design can be constructed with relative facility since non of the parts have extremely big dimensions, and many of the components are chosen from the catalogues, and are therefore standard and easily obtained. The most critical component of this proposed design is the air bearing, since the adequate functioning of the entire system greatly depends on how well the air bearing supports the belt and its load while reducing the friction. Given the importance of this component, the next chapter will be completely dedicated to it.

## Chapter 4

### 4 Externally Pressurized Air Bearing

#### 4.1 Introduction to Air Bearings

The engineering problem of rotating elements and their power loss due to friction has been an engineering concern for many centuries. A big step toward this problems minimization was taken with the invention of roller bearings (which replaced the plain bearings), reducing friction and wear considerably and pushing forward the known technical limits for rotating mechanical components. Obviously, the new developments in technology and machinery require a further step in the bearing technology evolution, in order to fulfill the necessities of faster and more accurate machines. This further development of the bearing technology has been taken based on air bearing technology.

Externally pressurized air bearings are mechanical elements with two very interesting characteristics that make them very attractive: they can offer a zero friction coefficient between tow surfaces, and they suffer no wear during their operation since the surfaces are not in direct contact. Taking advantage of the zero friction, air bearing have been used for applications where high precision or high speeds are required. Zero friction in air bearings allows reaching high speeds, and it also helps when high accelerations are required, since no slip occurs unlike the case of roller bearings. For instance, zero friction may be traduced into a high precision processes such as coordinate measuring machines or precision machine tools. Unfortunately, air bearings only became commercially available some years ago and so their use is still in growth, since their price is considerably higher than rolling bearings.

In the case of air bearings, the parts of interest are not in contact as in the case of roller bearings. Instead, a very thin layer of compressed air is used to create a fluid film between the moving parts with zero friction between them, and therefore there is no contact between the parts. Deleting the direct contact between parts gives air bearings their most outstanding advantages, since wear is no longer considered, lubrication is no longer necessary and friction reduces considerably. In fact, air bearing's wear is only driven by erosion, so it greatly depends on how clean the air supplied to the bearing is. Even more, when eliminating the lubrication requirements, the working environment is much cleaner since no oil is needed. Air bearings require a supply of compressed air which is forced to flow across orifices which must have a proper size in order to

restrict the flow according to the available air flow supply, but still maintaining a high pressure flow to create the fluid film. The air escapes constantly across the orifices and by directing it properly and homogeneously across the bearings surface it can create a fluid film with high stiffness and a low air consumption.

Friction is a major concern for many engineering problems, not only because the waste of energy and wear that it causes, but because it is a constantly changing parameter. Therefore, for situations in which a motion must be started or stopped with a high precision level, the changes between dynamic and static friction become a problem. However, when using air bearing static and dynamic friction coefficients become equal, and so it becomes easier to understand and control the problem, compared to what happens when using roller or plain bearings. Since an important part of power losses in machines are associated to friction, efficiency is greatly improved when using air bearings.

An important technical characteristic of air bearing is their stiffness. Common sense tends to make us think that an air bearing cannot offer an adequate stiffness, since the loads are being simply held by air. However, this is an erroneous assumption. For example, a circular air bearings working at 60 psi (4.14 bar) may have a stiffness of up to  $2 \times 10^6$  lb/in with a load of 1000 lb, which means that huge forces are required to cause very slight deformation. The stiffness of the bearings is greatly influenced by the air supply pressure, the surface area and the air gap height. In roller bearings, the loads are supported by the contact areas between the balls of the bearing and their race, so actually the force is distributed along a small contact area causing high stresses and consequently deformation. Instead, in air bearings, the load is supported by a much larger area, which explains why air bearings can have such a high stiffness though there is no direct contact present. However, air leakages around the edges must also be considered since they give rise to pressure gradients along the surface as the air exits from the orifices and expands around the fluid film. The pressure profile can be controlled by changing the location, size and amount of the orifices.

Air bearing are classified in '*orifice*' or '*porous media*' according to the way in which the pressurized air is supplied to the surface of the bearing. In orifice air bearings, the surface has a relatively small number of holes through which the air exits. In some cases, grooves are used in the surface to distribute the pressure along the surface. In the case of porous media, a porous material is used as the surface of the bearing so the orifices in the surface are much smaller but at the same time also more abundant, there are millions of them. Therefore the air pressure along the surface remains uniform along the entire area. The most commonly used material for the porous surface is porous carbon, which

adequately restrict the air flow across the surface and gives an almost flat pressure profile across the bearing's surface.



**Figure 32 - Porous Media Air Bearing**

As a rule of thumb, modern air bearings have proven to have an efficiency of nearly 50%, meaning that the actual pressure supporting the load is around half of the input pressure. Mostly, the efficiency depends on the geometry of the bearing, since small bearings will have most of their area near the borders, where most of the losses occur and therefore bigger bearings are expected to perform better. Considering the former ideas, in theory the performance of a bearing can be easily assessed as:

$$\text{Surface Area} * \text{Input Pressure} * \text{efficiency} = \text{Load Capacity}$$



**Figure 33 - Radial and Flat air bearing**

Air bearing can be commercially found in a variety of forms for different applications such as flat pads, air bushings or air bearing slides. The flat pads are the most efficient, and are also the most similar products respect the study case of the required air bearing for the rolling road. Among the standard available products the New Way air bearings company offers a 150x300 mm

rectangular flat pad. This product is sold as designed for a load of 11121 N, operating with an air supply at 60 psi (4.14 bar), condition at which requires an air flow of 4.2 liters per minute. At these operating conditions, the flat pad has an impressive stiffness of 1645 N/micron. We can therefore calculate the efficiency of the state of the art flat pads as a future reference.

$$efficiency = \frac{Load\ Capacity}{Area * Input\ Pressure} = \frac{11121}{(.15 * .3) * 413685} = 59.7 \%$$

The efficiency of air bearings can be affected by the presence of dust, oil or water, since they may cause drag and disturb the normal flow of air, and so the air supply must provide a relatively clean air. Modern porous material air bearings are designed to work at temperatures near the ambient one, and since there is no friction it is normally not a problem. However, considering the importance of the tolerances of the assembly of the bearings which may affect the air gap, the effect of temperature on the structure must be well considered. Also the surface finish of the part is important, and ideally should have a small roughness, since the roughness might change considerably the air gap when it is small.

The volumetric airflow on an air bearing is strictly dependent on the air gap size, and it has been proved to be a cubic function, so small gaps help to improve the efficiency and power required. In the case of orifice bearings, the differences in height along the air gap create instabilities, since at the places where the gap is larger the pressure reduces, and so air tends to escape along that way, reducing the pressure at the places with smaller gaps, where actually the pressure would be required. As a consequence special attention should be taken to the air gap, to control its height along the bearing in order to avoid serious losses.

This brief introduction to air bearing technology gave a general overview of this developing technology, which offers conceptually simple solution to common design concerns such as friction and wear. However, the use of air bearings has not been extensive since the efficient operation of these elements depends on the use of very tight tolerances, since the efficiency of the fluid film changes drastically with small changes in the gap between the bearing and the part as previously discussed, and therefore the cost can only be justified for certain precision applications. The state of the art air bearings are built with porous materials such as carbon, which allow the flow of the air through thousands of very small orifices, creating a homogeneous fluid film. However, given the particularities of this project, the bearing was designed as an orifice bearing, with which the shape of the rubber Poly-V belt could be easily manufactured.

## 4.2 Design of the Air Bearing Pad

Once the capabilities of air bearings was understood, it seemed feasible to build one able to provide pneumatic support to the rolling road belt and the load provided by the tire. Since the belt to support has a large amount of small ribs, it was not feasible to think about building the bearing with a porous materials, since the geometry is complex, and the wear of the belt could damage the pores of the material, and therefore an orifice bearing made of aluminum was considered as the best option. The next and most complex step was the design of the orifices, their diameter, amount and location.

The design of the air bearing was developed based on the available theory for the *Orifice Flow Meter* devices. These systems are used to calculate the fluid flow rate along pipes by measuring the pressure drop that is produced when the fluid passes through a small orifice of known size. The system is therefore simple, consisting of a plate with an orifice in the middle which is placed in the main pipe, and some pressure taps, located at known distances from the plate, used to measure the pressure drop. Given the upstream and downstream pressures ( $P_1$  and  $P_2$ ) and the diameters of the pipe and orifice ( $D_1$  and  $D_2$ ), it is then possible calculate the flow  $Q$  across the pipe, and with it the flow speeds of the fluid at each section of the pipe.

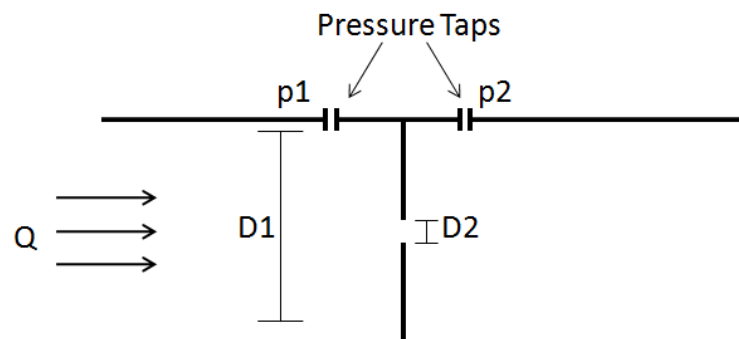


Figure 34 - Orifice Flow Meter Scheme

The orifice flow meter problem has strong similarities with the air bearing fluid dynamics, except the fact that the air bearing is not a pipe, and as a consequence it cannot be represented by a diameter dimension. However, the air bearing required to support the rubber belt is considerably big respect to the expected size of the orifices (expected to be in the range between 1 and 2 mm), and it was noticed that when  $D_1$  is much bigger than the orifice diameter, the results don't vary significantly with  $D_1$ , and so the orifice flow meter was considered to be a valid analogy. The equations describing the fluid dynamics through the flow

meters were used to calculate the air exit speed through the orifices based on the pressure difference across the bearing's surface and the orifice's diameter.

The orifice meter measures the flow based on the difference of pressure at both sides of the orifice. The device is therefore based on a plate with an orifice in the middle. The orifice causes an acceleration of the flow due to the area reduction, and therefore a pressure drop is caused which is equal to  $P_1 - P_2$ . The principle of this device is based on the Bernoulli equation:

$$\frac{P_1}{\rho} + \frac{v_1^2}{2} + gz_1 = \frac{P_2}{\rho} + \frac{v_2^2}{2} + gz_2 + \frac{\Delta P_{1-2}}{\rho}$$

A first approach assumes that the pressure loss across the orifice is negligible, which allows us to simplify the equation. Later in the calculations, the pressure loss is reconsidered in the equation by introducing a discharge coefficient. The change in altitude along the considered section of the pipe is also considered as negligible. The former considerations are introduced in the previous Bernoulli equation as:

$$\Delta P_{1-2} = 0$$

$$gz_1 = gz_2$$

The flow velocities before and after the orifice plate can be expressed in terms of the volumetric flow rate  $Q$ , and the section areas (calculated based on the diameters) as follows:

$$V_1 = \frac{4Q}{\pi D_1^2}$$

$$V_2 = \frac{4Q}{\pi D_2^2}$$

By deleting the neglected term and replacing the expressions for the velocities  $v_1$  and  $v_2$ , a new equation is obtained. It is now possible to calculate the pressure drop  $P_1 - P_2$  from the Bernoulli equation:

$$\frac{P_1 - P_2}{\rho} = \frac{1}{2} (v_2^2 - v_1^2) = \frac{1}{2} \left( \frac{16Q^2}{\pi^2 D_2^4} - \frac{16Q^2}{\pi^2 D_1^4} \right) = \frac{16Q^2}{2\pi^2} \left( \frac{1}{D_2^4} - \frac{1}{D_1^4} \right)$$

In the former equation the only unknown term is the volumetric flow rate  $Q$ , since the pressures and diameters are all known. Consequently, solving for the volumetric flow rate  $Q$  we obtain:

$$Q = \sqrt{\frac{1}{1 - \left(\frac{D_2}{D_1}\right)^4}} \frac{\pi D_2^2}{4} \sqrt{\frac{2(P_1 - P_2)}{\rho}}$$

Up to this point, we have considered that the pressure drop across the orifice is negligible, and that the density of the fluid remains constant when flowing across the section reduction. It is then necessary to introduce a coefficient of discharge “ $C_d$ ” to adjust the formula for the actual pressure change, and an expansion coefficient “ $e$ ” for the change in density. In order to simplify the equation, the first square root term can be called  $E$ .

$$E = \sqrt{\frac{1}{1 - \left(\frac{D_2}{D_1}\right)^4}}$$

With the former simplification, and introducing the still unknown terms of the discharge and expansion coefficients, the volumetric flow rate equation takes its final expression:

$$Q = C_d e E \frac{\pi D_2^2}{4} \sqrt{\frac{2(P_1 - P_2)}{\rho}}$$

The expansion coefficient for air and other gasses can be easily calculated based on the pressure drop  $\Delta P$ , the isentropic coefficient  $k$  (which for air is equal to 1.4) and the ratio between the diameters of the orifice and the pipe  $\beta$  ( $D_2/D_1$ ).

$$e = 1 - (0.41 + 0.35\beta^4) \frac{\Delta P}{kP_1}$$

The use of the Flow Meter theory requires the calculation of a discharge coefficient to adjust the theoretical values to the real ones according to the losses that might be present, which is an analog situation to what happens in an air bearing, where the orifices act as nozzles. Many different approaches have been developed to understand the dynamics of a compressible fluid like air through orifices, and most of them lead to discharge coefficients ranging from 0.6 to 0.8



calculated by means of empirical formulas (as in [8]) which are obviously limited to specific operation ranges and characteristics of the orifice, but still the discharge coefficient values does not significantly vary between the different approaches.

For this particular case, the calculations of the discharge were based in a standard formula used for Orifice Flow Meters. Back in 1991, the orifice plate discharge coefficient calculation was standardized by the means of the ISO 5167. The discharge coefficient depends on the ratio between the main diameter of the pipe, and the diameter of the orifice, and the type of pressure taps used (among three possible types). Therefore, the Discharge coefficient can be calculated according to the ISO standard as:

$$C_d = 0.5959 + 0.0312\beta^{2.1} - 0.1840\beta^8 + 0.0029\beta^{2.5} \left(\frac{10^6}{Re}\right)^{0.75} \\ + 0.0900 \left(\frac{L_1}{D_1}\right) \left[\frac{\beta^4}{1 - \beta^4}\right] - 0.0337 \left(\frac{L_2}{D_1}\right) \beta^3$$

In the former formula for the discharge coefficient, the terms  $L_1$  and  $L_2$  are constants given by the type of taps used measure the pressure drop. For the case where the pressure is measured just after and just before the orifice, known as corner taps,  $L_1=L_2=0$ , while for taps measuring the pressures at a distance of one inch from the orifice,  $L_1=L_2= 0.0254/D1$ . As in the case of the expansion coefficient, the term  $\beta$  represents the ratio between the orifice and the tube diameters, and is therefore smaller than 1. By observing the formula and considering  $\beta$  is smaller than one, we notice that the discharge coefficient will be around 0.6 and will just vary slightly regardless the values of the considered parameters.

By making an analogy between the orifice plate calculations, and the actual required situation with the externally pressurized air bearing, it was possible to set the ideal values of the main design parameters of the bearing such as the number of orifices and their diameter. Ideally, an air bearing should have a large amount of small holes well distributed along the surface able to provide an homogeneous air flow at high speed and pressure to create the pressurized fluid film that supports the load. The main restrictions of the bearing design for the RuotaVia are the number of holes that could be done, in order to make the manufacturing process feasible, and on the other hand, the size of the holes. Very small holes could cause big pressure losses and manufacturing difficulties, while big holes would reduce the number of them, but affecting the homogeneity of the pneumatic support. Therefore an adequate number and size

for the orifices had found, and these two variables were linked together by the available volumetric flow rate that the air compressor can provide at the maximum operation pressure.

The RuotaVia Test facility laboratory (L.A.S.T.) has an INGERSOLL-RAND air compressor of the model ML37 GD, which is rated to work at a maximum pressure of 7.5 bar with an air flow of 6.3 m<sup>3</sup>/min. With the previous values, and considering that some losses are present due to the long way between the compressor and the facility, the number of orifices and their sizes were chosen. However, in order to adequately tune the parameter values, an experimental test was developed, building a smaller pressurized air bearing and determining if it was capable of supporting a load and allow the belt to slide easily over the bearing.

In order to run the calculations, a 6.5 bar input pressure was set, since some losses are present between the compressor and the laboratory. An opposing pressure ( $P_2$ ) of 3 bar was set as to simulate the load on the belt caused by the tire. Considering the size of the air bearing, and the 3 bar pressure, the belt should theoretically be able to support a load of around 2300 N, which considering an expected efficiency of nearly 50% should be more than enough to support the 1000 N that were considered as the load over the rolling road. With these values, some preliminary results indicated that the orifices diameter should be between 1 and 1.5 mm in order to obtain good exit velocities and a large number of orifices (to distribute them homogenously across the surface) while not exceeding the available volumetric flow capacity of the air compressor.

### 4.3 Air Bearing Test

Based on the preliminary results obtained analytically, the air bearing solution seemed a feasible solution for supporting the rubber belt while reducing considerably the friction between the belt and the support. However, in order to assess the validity of the results and assumptions, an experimental test was done. A small air bearing with the orifice diameters found with the mathematical model was manufactured to perform testing in how it could support a loaded rubber belt, and allow it to slide with a small resistance.

Since a rubber belt from the exact type as the one chosen for the rolling road was not available for this experimentation, a common automobile belt was used. The chosen belt was a 6 PK 1255, meaning it had 6 ribs, a PK profile and an

effective length of 1255 mm. The PK profile has a 3.56 mm distance between ribs, and a 40 degree angle in the ribs, and therefore was slightly smaller than the L profile chosen for the actual belt of the rolling road, which of course also has many more ribs. However, it was similar enough as to obtain some insight of how the air bearing could perform.

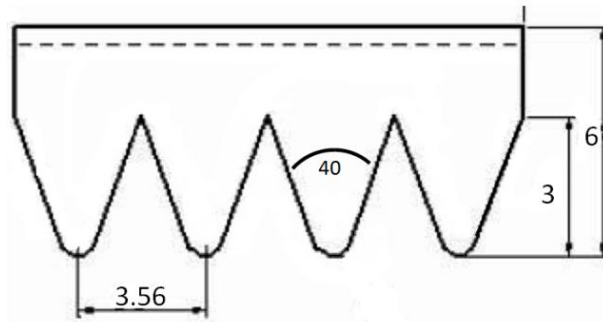


**Figure 35 - PK Belt Profile**

As previously discussed, modern porous material flat pad air bearings have efficiencies arriving up to 60%, and therefore lower efficiencies are expected for orifice air bearings like the one here considered. However, given the Poly-V cross section of the rubber belt, the air and pressure losses are expected to be reduced compared to a traditional flat pad bearing. The air cannot easily flow toward the sides of the belt due to the ribs, and therefore the air will only be able to flow towards the front and rear of the air bearing, which is expected to generate a significant increase in the efficiency. However, the ribs also increase the contact area between the belt and bearing and so the friction between belt and bearing can increase compared to the situation of having a flat pad bearing, and therefore we expect a negative effect of the ribs in the efficiency, but also compensation due to the air flow in only one direction.

A small air bearing (45x100 mm) was manufactured in aluminum with the adequate profile specified for the pulleys of a PK Poly-V belt. Compared to the dimensions of the bearing of the rolling road, the area where the test belt is supported is around 37 times smaller. The experimental bearing was designed with 17 orifices having a 1.3 diameter, with which an exit air speed of around 144 m/s was expected according to the theory. The orifices were distributed symmetrically along the bearing, and in order to reduce the losses, they were concentrated in the 3 central ribs of the rubber belt so less air would escape through the sides. In order to simplify the manufacturing of the bearing, the air chamber under it was done with long radius rounded edges so it could be easily done with a milling process. Finally, 6 threaded holes for M6 bolts were done in order to close the air chamber with a rubber gasket and an aluminum plate having the compressed air inlet connection. For the case of the actual bearing,

the chambers will have a rectangular shape, so that orifices may be located closer to the borders in a more homogeneous way.

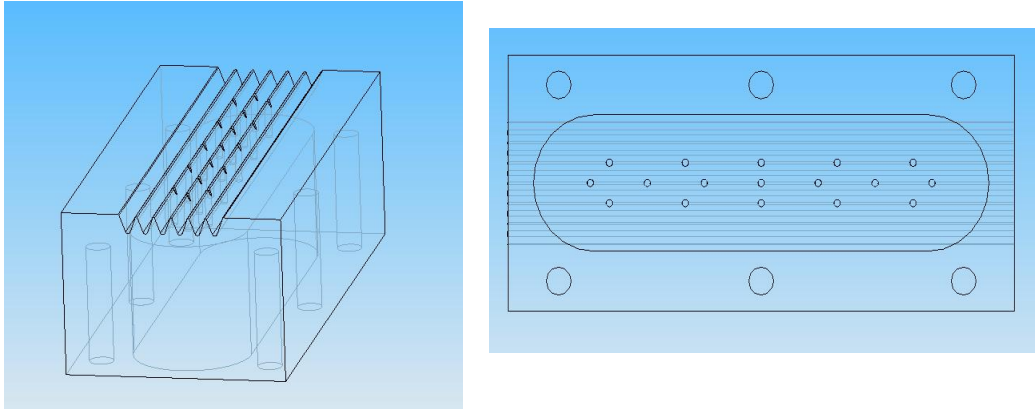


**Figure 36 - Model Air Bearing for Test**

The objective of this experimental testing was to determine the capability of the designed air bearing to actually give a pneumatic support to the rubber belt, allowing it to easily slide (by reducing the friction with the air film) over the bearing while loaded with different masses. The testing was done under the basis of a low cost assessment of the performance of the bearing's performance, reason for which a used rubber belt was used (though the profile was slightly different for the one that will be used) and no instruments to precisely measure the performance were available. Even though the testing method was quite simple and economic, the experimental setup was good enough to provide a qualitative analysis of the performance of the bearing under different loads and pressures, giving enough information about the behavior of the belt, the load and the bearing useful to further develop the air bearing design for the rolling road.

Once the air bearing had been adequately closed with the gasket and bolts and no air leakages were present, it was firmly supported and constrained with a press, giving special attention to fix it in a completely horizontal position. Once the bearing was set, the PK rubber belt was cut to obtain shorter segments of belt of around 30 centimeters. Finally, a variety of steel masses with weights ranging from 100 to 8000 grams were used to simulate the load over the belt, and determine the actual capacity of the air bearing to support the belt with its load.

The experimental procedure consisted in locating the piece of belt over the bearing, loading it with a mass and qualitatively determining how good, bad or poor the bearing performed in allowing an effort free back and forth displacement of the belt with the load over it. The process was repeatedly done

for each of the different available masses since the results were totally qualitative, the testing was done for hours in order to eliminate the variability in the judgment that could arise from such a method. With each available mass the compressed air input pressure was varied along the available range, from 1 to 6.5 bar (the maximum reached at the facility). Finally, the minimum required input pressure for the belt to move freely for each load was determined.



**Figure 37 - Air Bearing Experimental Test Setup**

Before introducing the experimental results, we must mention the main complications and difficulties that were found during the test, which must be considered for interpreting the results, for future experimental approaches and for the final design of the real full size air bearing. A minor inconvenient was the presence of lubricant in the compressed air supply which became evident in the air bearing's surface after some minutes of testing. The effect of the oil is hard to assess, but theory indicates its presence in the orifices causes drag in the air flow and a consequent pressure drop from the compressed air. During the testing the lubricant was cleaned continuously to remove its effect from the testing results, but should be a concern for the full size bearing which will not be so easy to clean often.

Besides the oil concern, a bigger problem came from the available masses used to load the belt, which had very different geometries that in many cases were not easily balanced over the moving rubber belt (as seen in figure 38), which was only 21 mm wide, compared to the 338 mm width of the real size bearing. The bearing was also in many cases larger than the bearing, so inevitably the load would eventually lean toward the bearing's edge, were no pressurized air supply was available, and therefore the free sliding of the belt were affected as a direct

contact between the load and the bearing occurred. We must therefore remark the importance of applying the load adequately, not allowing it to apply excessive pressure in those places where the fluid film is weak such as the bearing borders.



**Figure 38 - Air Bearing and Belt Supporting a Steel Mass**

The positioning problem with the load was also useful to understand the importance of an adequate alignment between the belt and the bearing, which should be as parallel as possible to avoid additional friction. Very small changes in the position of the load over the belt caused significant increases in the force required to slide the belt. Therefore, those masses having a width similar to that of the belt were very easily placed over the belt and the belt could easily slide over the bearing's surface. Instead, those masses with a bigger width to that of the belt were very hard to position over the belt and usually tilted to a side increasing the friction, as the load was then not only acting on the belt. However, the air bearing proved to be capable of supporting all the masses and make the belt slide frictionless, provided an adequate location of the load over the belt was achieved. Considering that the real size air bearing will have rectangular chambers and not oval shaped as the experimental one, it will be possible to locate orifices closer to the border, and this problem should be reduced, also considering the load of a tire in the rolling road will be concentrated in the center, so loads in the border should not appear often.

The graph in figure 39 resumes the behavior of the air bearing with the different masses, showing the minimum input pressure that was required to slide the belt along the air bearing's surface with a very low effort. A non linear behavior between the weight and the pressure was observed, in fact, the results are well represented by a logarithmic equation, so the larger the weight, lesser the

required pressure is. The results obtained lead to an analysis of the behavior of the state of the art commercial air bearings. In commercially available catalogues of flat pad air bearings, the ideal load for each bearing is given, so that the air gap has an optimal value that guarantees supporting the load and a given stiffness. The graph in figure 40 was done based on the product catalogue of New Way Air Bearings, and shows the ideal load for rectangular flat pad air bearings of different sizes.

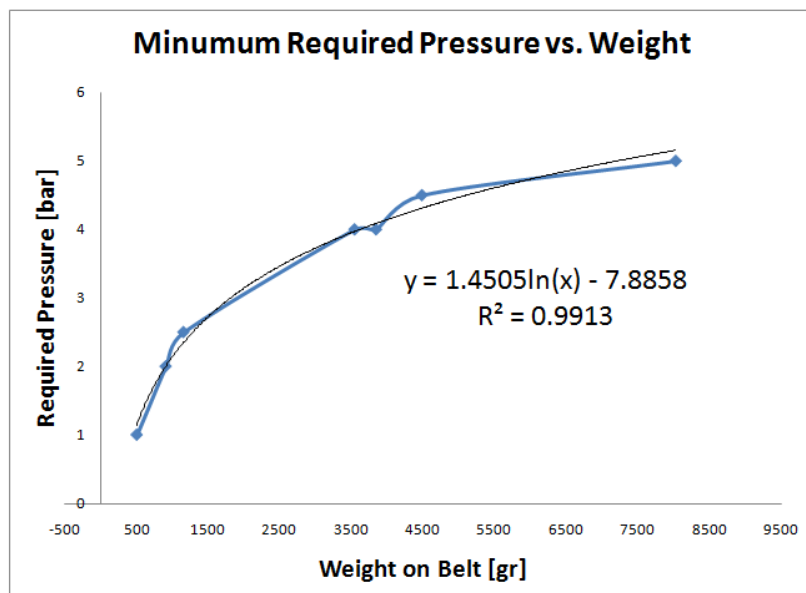


Figure 39 - Experimental Air Bearing Performance

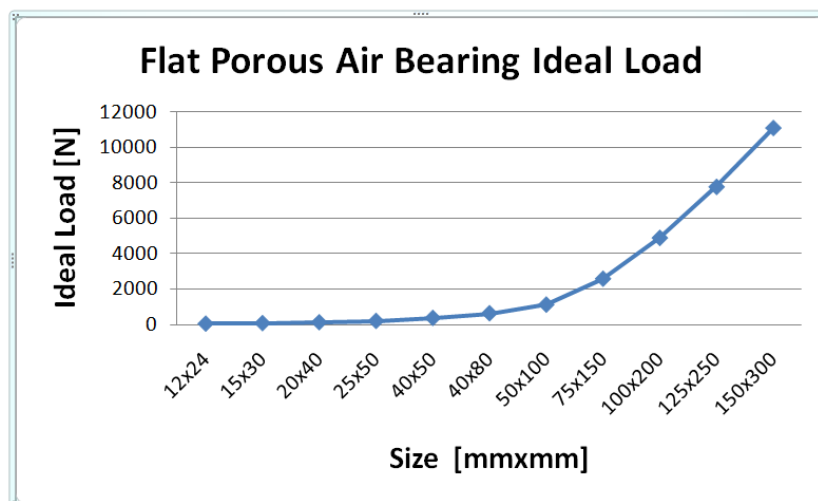


Figure 40- New Way Flat Pad Air Bearings Ideal Load

The graph shows that for state of the art air bearings, the load capacity increases exponentially with the size and in fact, the stiffness has the same behavior. When calculating the efficiency of the same rectangular flat pad bearings, we notice that at a constant input pressure (60 psi), the load that can be supported by the bearing increases as the bearing's size increases. This performance behavior gives an insight to understand the results obtained during the experimental test of the bearing, and gives a positive signal toward the expected behavior of the full size air bearing for the rolling road.

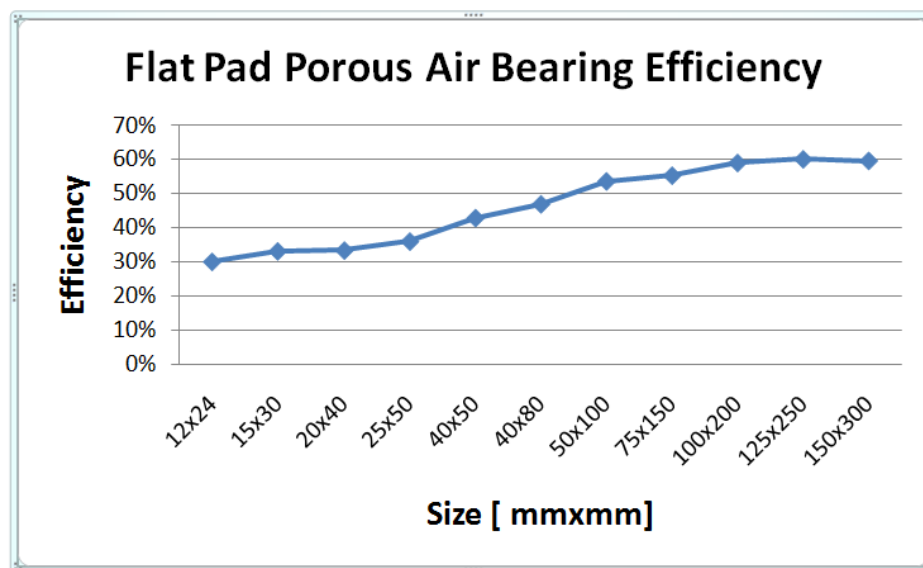


Figure 41 - New Way Flat Pad Air Bearings Efficiency

Higher loads generate smaller air gaps between the bearing and the sliding surface, and as previously mentioned, smaller fluid films increase the stiffness of the bearing. When the fluid film is smaller, the pressurized air cushion formed by the fluid film can easily keep the pressure, but it becomes harder as the gap increases, requiring a much higher air flow. Considering the former, it is possible to explain the experimental results and the non linear increase of the required pressure with the load on the belt. Therefore, for small loads, the air bearing proved to be quite inefficient, since the air could easily lift the belt making it float in an unstable way, which for sure generated contact between the bearing and the belt, making it hard to move. Instead, for higher loads the belt was much more stable, which probably created a more homogeneous fluid film and therefore the bearing behaved much better.

During the testing, it was evident that the ribbed section of the belt does not allow the air to escape through the sides of the bearing as had been expected, and therefore all the air flow exited the bearing along the V shaped grooves of



the bearing. Another important detail obtained during the testing, was the importance of the surface finish of the air bearing. Since the belt is a quite flexible element, inevitably there will be spontaneous contact between the belt and the bearings surface, and so sharp edges on the bearing can stick on the belt damaging it and increasing the resistant force during the contact.

The greatest load that was possible to put over such a small belt was an 8 kg steel block, which was possible to slide with a slight effort while feeding the bearing with a 5 bar input pressure, though it was hard to position it over the belt since it was about 3 times wider than the belt. In fact, the results show an asymptotical tendency of the required input pressure to approach a value around 5 bar as the load increases. Therefore, considering the bearings efficiency is expected to increase as the bearing area increases, the air bearing should be able to perform adequately giving support to the rolling road, and in normal conditions should not be necessary to use the maximum available input air pressure of 6.5 bar. As a matter of fact, when feeding the bearing with an excessive pressure, the air gap will increase, increasing at the same time the pressure losses.

Considering all the information gathered from the testing, the final design for the air bearing was determined. The testing successfully proved that the compressed air can create a fluid film able to support the ribbed surface of the rubber belt. Even more, the testing showed that available air pressure exceeds the required performance, but the necessity of a homogeneous pressure distribution along the surface was the most outstanding conclusion. Therefore, it was decided to slightly decrease the diameter of the orifices (passing from 1.3 mm to 1.2) in order to be able to make more of them without exceeding the available flow rate provided by the air compressor. With this change, 540 orifices can be done, which would require 5.3 cubic meters of air every minute, out of the 6.3 available according to the compressor's catalogue. With these specifications, there would be one orifice for every 110 mm<sup>2</sup> of the bearings surface, which is slightly higher than the experimental case (1 orifice for every 123 mm<sup>2</sup>).

The air bearing surface area was divided in 12 independent chambers, separated between them by 4 mm walls. Since the chambers are independent, the air supply pressure can be changed individually in each of them, and therefore it is possible to adjust the air supply according to the distribution of the load on the belt, in order to obtain a homogeneous pneumatic support along the entire surface of the belt. Vehicle tires do not generate a completely vertical and centered load, since the suspension's setup introduces the camber and caster angles, which vary the direction of the loads. Additionally, the pressure profile

generated by the tire on the road locates the resultant force slightly ahead of the center, generating a torque that opposes to the rotation. Considering the variability of the pressure distribution over the belt, the pressure on each chamber can be varied to optimize the performance.

In an attempt to predict the possible sources of malfunctioning and if possible make the required corrections with relative facility, some strategic changes were done to the concept of the air bearing. Firstly, with the scope of simplifying the manufacturing of the bearing in case some part had to be replaced, it was decided to build it in three different parts, instead of two. The original concept of the air bearing was to build it from a single plate of metal, milling the grooves for the pulley and the air chamber, and drilling the orifices, and finally close the chambers with a second plate. Instead, it was considered more adequate to split the air bearing in two 19 mm thick plates (in order to manufacture them from a 200mm thick standard plate). The first plate has the grooves for the belt, the orifices for the compressed air to exit, and 20 threaded holes for M6 bolts that close the air bearing. The second plate has the walls that separate the air bearing surface into the 12 independent chambers, and it also has the four holes for the cylinder that support the air bearing between the belt.

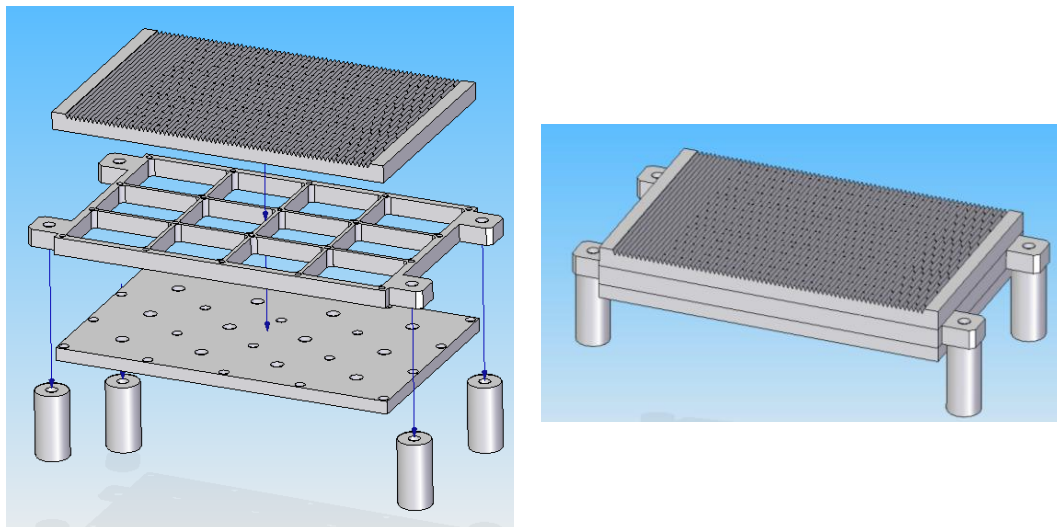


**Figure 42 - Air Bearing Definite Concept**

Due to the considerable thickness of the primary plate of the air bearing, it resulted quite difficult to drill such small orifices (1.2 mm of diameter) across the entire thickness of the plate. Therefore it was necessary to pre-drill some bigger orifices (4 mm diameter and 10 mm deep) in order to facilitate the drilling. Starting from the acquired information during the testing, special

attention was given to the distribution of the orifices along the surface of the bearing, in order to make it as homogeneous as possible and avoid weak points where the friction could be increased. A total of 540 orifices were distributed along the bearing's surface, in such a way that every groove has at least 7 orifices.

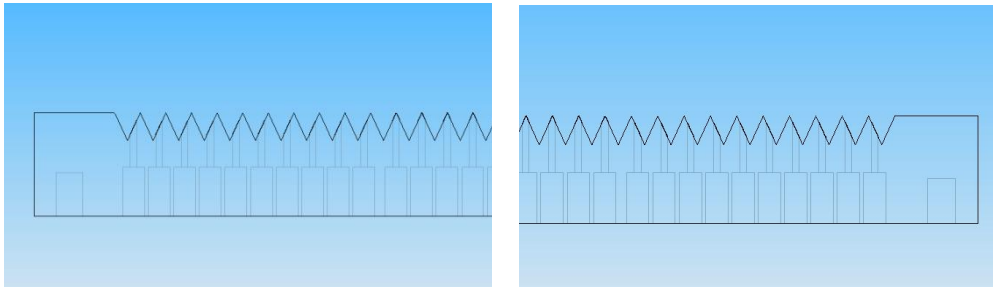


**Figure 43 - Detail of Orifice Location**

Besides the distribution of the orifices, their location respect to the ribs was also considered in an attempt to optimize the bearings response when subjected to lateral forces. Therefore, the first rows of orifices at the extreme left and right chambers were displaced by  $\frac{1}{4}$  of the pitch to the left and right respectively. In this way, the air exiting from these displaced orifices will approach the belt in such a way that the thrust will produce a force in the belt with a lateral and a vertical component. Figure 43 shows a cross section of the left and right chambers, where the rows of displaced orifices can be seen closer to the edges, while the rest of the orifices are located at the top of the ribs.

Although it is hard to determine if the lateral force generated by this air flows will be enough to totally support the lateral forces that the tire will cause in the belt, at least it should help the belt to return immediately to its original position after the lateral load is applied. For the previous statement we must consider that lateral forces are only expected to appear during separated time short instants (i.e. as when the opposite tire passes over a cleat exiting the complete suspension) and therefore the inertia of the system will keep it rotating at the adequate speed, while the displaced orifices will help the belt to return to its central position once the load dissipated. All the rest of the orifices across the bearing were located at the top of the bearings ribs, where the belt tends to contact first with bearing, and therefore the smallest gap between the belt and bearing is located in there, reducing the pressure losses.

## Chapter 5

### 5 Conclusions

The increasing importance of understanding the behavior and response of modern vehicles has made the suspension systems and tires testing methods an important tool for improving the vehicle's safety, comfort and control. Due to the different experimental approaches used for testing either tires or suspensions, test rigs have been usually designed separately according to the specific testing parameters of each approach. Usually, tires are tested under high speeds and loads, especially in the lateral direction. Instead, suspension systems are often tested while the tires remain static as in Suspension Parameter Measurement Machines, where the testing is based in forces and displacements generated by actuators under the tires. Given the state of the art situation concerning tire and suspension testing, the RuotaVia Test Rig belonging to the Laboratory for the Safety for Transport (L.A.S.T.) of Politecnico di Milano is an outstanding facility able to perform unique experimental procedures.

Among the different experimental tests that can be done in the RuotaVia facility, is the vibration behavior analysis of suspensions, in which the tire runs over the rotating steel drum and is periodically exited when passing over a cleat. For this type of test, better results are expected when both tires of an axle are simultaneously rotating. When both tires can rotate during testing, the vehicle's behavior in the test rig gets a better approach to the real on road performance of the vehicle, since more elements such as the tires, shafts and sway bars are operating in their real conditions. Since the original concept of the RuotaVia test rig can only drive one wheel, a mechanical system is required to support and make the opposite tire rotate simultaneously with that over the steel drum. Based on the required testing parameters such as the loads and speeds, different types of mechanical systems were considered, and that one which most adequately fitted the test rig and the desired performance and was proposed for implementation in the near future after a detailed description and analysis of the proposed system was presented.

During the brain storming process previous to the design, different options were considered to support and rotate the vehicle's wheel. The first considered idea was based in a small rotating drum, to drive the tire in a similar way as the RuotaVia drum does. However, this type of approach was ruled out due to the limited available space at rig and because of the necessity of simulating the rotation of the tire over a flat surface, which cannot be done with small radius

drum. The design process was then taken toward the rolling road technologies, which are a state of the art solution for tire testing machines and applications as wind tunnel rolling roads. Following the state of the art test machines, a steel belt rolling road was studied as a possible solution to support the wheel. Unfortunately, metal belts only perform adequately when used with big pulleys, and therefore the overall system resulted too big, difficult to build and with low operational flexibility, since it could hardly be adapted for future changes.

The design process was finally taken toward a rolling road based on POLY-V rubber belt, which could be fitted in much smaller structure to support the tire and drive it to speeds up to 100 km/h, as required when studying the vibration behavior of suspensions. Rubber belts are not capable of supporting high loads located in the span between the pulleys, so it was necessary to provide a supporting surface for the belt just under the section where the tire will be in contact with the belt. Any supporting surface would generate high resistant forces due to the friction with the rubber belt, so an externally pressurized air bearing pad was designed to support the belt with a compressed air fluid film.

Externally pressurized air bearing are a state of the art solution to reduce friction in high precision applications but their use for a similar application was not documented, and therefore an exhaustive research in how to model and adapt it to a ribbed rubber belt was done. The air flow across the air bearing was modeled based on the *Orifice Flow Meter* devices theory, which allowed the calculation of the air speed while exiting the bearing, in order to calculate the required flow to maintain the air pressure at the air gap supporting the belt. An experimental test was done to assess the actual capability of the compressed air of supporting a ribbed belt. The results of the experiment in the scaled air bearing gave enough evidence to affirm the full size bearing can adequately operate in the rolling road supporting the belt and allowing it to slide easily over the air bearing's surface.

According to the acquired information during the test, a careful tuning of the system after the construction will be of vital importance for its optimal performance. The air pressure employed at each of the 12 air chambers (according to the load distribution) will be important to maintain a homogenous air film across the bearing's surface, reducing friction and making the belt slide smoothly. The assembly tolerances must also be kept under control, specially the parallelism between the bearing's grooves and the belt ribs to guarantee the in order to minimize the undesired contact between the belt and the bearing's surface. Once the rolling road is adequately tuned, it will take the RuotaVia test rig a step further in the experimental analysis of the behavior of vehicle suspension systems.

## Bibliography

- [1] F. Giorgetta. On the testing of vibration Performance of Road Vehicle Suspensions. Society for Experimental mechanics. 2007.
- [2] G. Mastinu, M. Pennati. Design and Construction of a Test Rig for Assessing Tyre Characteristics at Rollover. Society of Automotive Engineers, Inc. 2002.
- [3] Cinghie e Pulegge POLY-V. Catalog 1208X. Poggi Trasmissioni meccaniche s.p.a. Edition 2008. <http://www.poggispa.com/>
- [4] Design Guide and Engineer's Reference for Metal Belts. Belt Technologies Inc. Europe. 1999. [www.belttechnologies.com](http://www.belttechnologies.com)
- [5] 180-mph Rolling Road Wind Tunnel. Windshear Inc. <http://www.windshearinc.com>
- [6] Tire Testing. VMI Group. [www.vmi-group.com](http://www.vmi-group.com)
- [7] Air Bearing Application and Design Guide. NewWay Air Bearings. Aston, Pa, USA. January of 2006. [www.newwayairbearings.com](http://www.newwayairbearings.com)
- [8] Belforte G. Discharge Coefficients of Orifice-type Restrictor for Aerostatic Bearings. Department of Mechanics, Politecnico di Torino. ScienceDirect July of 2006.
- [9] Wen-Jong Lin. Modelling of an Orifice-type Aerostatic thrust Bearing. Singapore Institute of Manufacturing Technology. ScienceDirect.
- [10] G. Mastinu. Nuovo Impianto Sperimentale per Studi sulla Sicurezza Attiva del Veicolo. Department of Mechanics, Politecnico di Milano. 2005.
- [11] G. Mastinu, M. Pennati. Technological Issues of the Ruota Via Test Rig of the Laboratory for the Safety of Transport at Politecnico di Milano. Department of Mechanics, Politecnico di Milano. 2005.
- [12] Lingyuan Kong. Robert Parker. Mechanics and Sliding Friction in Belt Drives With Pulley Grooves. Department of Mechanical Engineering, Ohio State University. March of 2006.

- [13] J.W. Roblee, C.D. Mote Jr. Design of Externally Pressurized Gas Bearing for Stiffness and Damping.
- [14] Joseph E. Shigley. Mechanical Engineering Design. McGraw Hill 2004. Seventh edition.
- [15] Akpobi, J.A.; Ovuworie, G.C. Computer–Aided Design of the Critical Speed of Shafts. Production Engineering Department, University of Benin, Benin City, Nigeria. December of 2008.

## Figure References

- [1] ,[2] G. Mastinu, M Pennati, M Gobbi. Technological Issues of the RuotaVia Test Rig of the Laboratory for the Safety of Transport at Politecnico di Milano.
- [6] Taken from *Anthony Best Dynamics* website. <http://www.abd.uk.com>
- [7] Taken from *VMI Group* web site. Tire testing. <http://www.vmi-group.com>
- [8] Taken from *MTS Systems Corporation*. MTS Flat-Trac III CT tire test system brochure. <http://www.mts.com>
- [9] Taken from *Windshear Corporation* web site. <http://www.windshearinc.com/>
- [14] Taken from *SKF Power Transmission* web site product catalogue. <http://www.skfpt.com>
- [15], [16] Taken from Belt Technologies Europe. Design Guide and Engineer's Reference for Metal Belts. [www.belttechnologies.com](http://www.belttechnologies.com)
- [17], [18], [20], [23] Taken from *Poggi Trasmisione Meccaniche*. Chingie e Pulegge POLY-V Catalogue 1208X. <http://www.poggispa.com>
- [29] Taken from *SKF* web site bearings product catalogue. Angular Contact Bearings. <http://www.skf.com>
- [32], [33] Taken from *NewWay Air Bearings* web site. Air Bearing Application and Design Guide. January of 2006. <http://www.newwayairbearings.com>

## Appendix 1

### 1 Belt Support with Rolling Cylinders

Considering the unknowns concerning the actual performance of the air bearing for supporting the rubber belt previous to its construction, an additional supporting method was considered as an alternative solution in case the desired performance was not achieved with the pneumatic support of the externally pressurized air bearing pad. The new considerate alternative was studied with the objective of simply replacing the air bearing in case it would not work properly, and therefore the new alternative should be able to fit in the previously considered structure, without modifying the belts or pulleys.

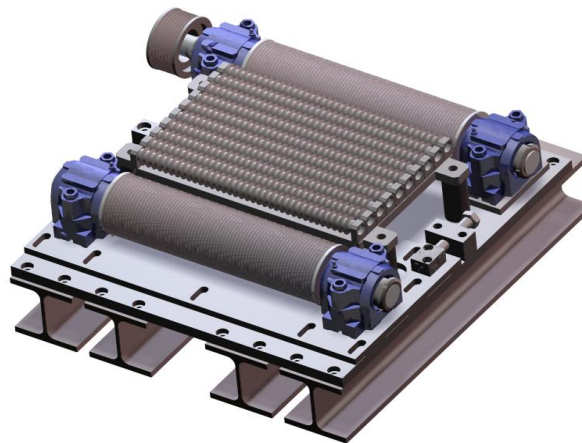


**Figure 44 - Alternate Belt Supporting Method with 10 Supporting Cylinders**

In a first attempt to design the alternate supporting system, a series of 10 rolling cylinders tightly assembled together was considered. Such a big number of cylinders was considered in order to provide an almost flat supporting surface over which the POLY-V belt should pass. In order to provide a very homogeneous supporting surface, the supporting rolling cylinders were designed in such a way that each one of them has a rib to guide the belt every 9.4 mm, which is twice the pitch of the rubber belt (4.7 mm). In this way, the cylinders have the ribs required to track the belt and keep it in the central position, but at the same time the assembly can be done in a compact way, and the contact area between the belt and cylinders is reduced which also reduces the contact friction. Therefore, two types of rolling cylinders are required, in which the ribs for the belt are displaced by 4.7 mm respect to each other. By using both types



of cylinders assembled in an alternate sequence, the assembly is compact, and the created surface is relatively flat. The alternative supporting method requires no changes in the previously described structure, besides manufacturing a supporting plate for the bearings that support the cylinders, the bearing supports and the cylinders themselves.

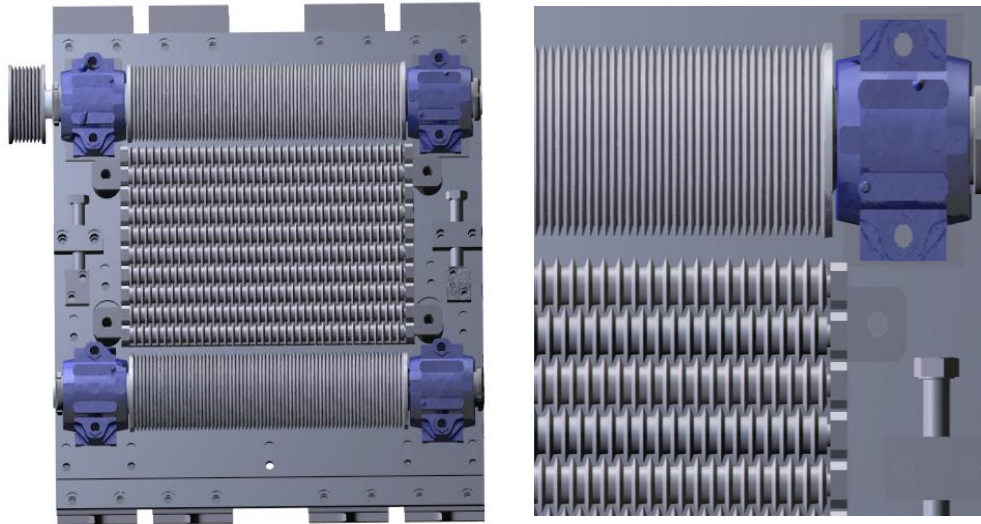


**Figure 45 - Rolling Cylinders Assembly Detail**

The ideal flat supporting surface is obtained by using rolling cylinders with the smallest possible diameters, however, given the high speed at which the rubber belt is driven, small diameter imply a very high rotational speed of the cylinders. In order to fit 10 cylinders, and according to the available space between the rolling road pulleys, the external diameter of the cylinders would be 28.5 mm. Assuming the belt contacts the pulley at the top of the cylinders ribs, and considering the belt's speed (100 km/h), the cylinders would rotate at a speed of:

$$w_{supports} = \frac{v}{\left(\frac{D_e}{2}\right)} = 1949 \frac{rad}{s} = 18611 \text{ rpm}$$

A rotation speed of 18611 rpm means that the shaft will rotate at a frequency of 310 Hz. At such a high rotation frequency, the phenomenon of the critical rotation speed of shafts becomes important and must be considered by the designer. The critical rotation speed is defined as the minimum rotation speed at which the natural frequencies of a shaft (or any similar rotating element as could be a gear) are excited. The critical speed is a result of the slightly eccentric center of gravity of the rotating element due to a deflection. Therefore, even a shaft with no external loads applied has a critical speed as a result of the

deflection caused by its own weight. As the actual rotation speed approaches the critical speed (or one of its harmonics), the natural frequencies are excited generating a resonance effect that increases the vibration of the system and make it unstable.

The increased deflection due to the resonance at the critical speeds is known as *whirling*. The instability caused by driving a shaft near its critical speed is a dangerous operational situation as it seriously compromises the shaft's reliability. Therefore, as a rule of thumb ([14]), often the first critical speed is desired to be at twice the operating speed. However, the critical speed varies with the loading conditions, which influence the shaft's deflection and therefore the critical speed lowers. Besides the critical speed of the shaft and its own vibration modes, the effect of the bearings and their supports also affect the vibration modes, and therefore the shaft's vibration is not a simple phenomenon. In general, the critical speed corresponds to the natural frequency of transverse vibrations of the unloaded shaft. For a constant diameter shaft simply supported over two bearings [16], the first critical speed can be calculated as:

$$\omega_1 = \left(\frac{\pi}{l}\right)^2 \sqrt{\frac{EI}{m}} = \left(\frac{\pi}{l}\right)^2 \sqrt{\frac{gEI}{A\gamma}} \quad \left[\frac{rad}{s}\right]$$

In the critical speed formula,  $\gamma$  is the specific weight,  $m$  the weight per unit length (kg/m),  $I$  the moment of inertia and  $A$  the cross section area of the shaft. By considering the minimum constant diameter of the supporting cylinders (18.28 mm at the base of the ribs), the first critical speed would be found at 18109 rpm for an aluminum shaft, which is under the operating speed. Since the critical speed is strongly dependent in the material of the shaft, a slight improvement in the critical speed is achieved by manufacturing the supporting cylinders with steel, since the critical speed increases proportionally to the square root of the elastic modulus. However, the critical speed is also inversely proportional to the density, as the initial deflection is increased by the shafts own weight. Considering a steel shaft, the critical speed value increases to 18321 rpm which is still too close to the operating speed. In fact, the use of steel is desired not only for the higher achievable operating speed, but in this case also for the higher weight of the supporting cylinders, which will therefore have a higher inertia to help maintain a constant rotation speed of the belt when it is subjected to the instantaneous forces applied when the opposite tire passes over the cleats. For reference purposes the critical speed of the pulleys of the rolling road (which are made from aluminum) were calculated resulting in a critical speed over 92000 rpm when considering the 93 mm diameter, or 35000 rpm when just considering the 35 mm of the pulley shaft.

The critical speed frequencies calculated analytically were compared to the natural frequencies of the cylinders found by means of Finite Element analysis with the ABAQUS software. The results obtained by FEM agreed with the analytical results, and as expected (according to [14]) the analytical formula slightly overestimates the critical frequency. In example, for a 18.28 mm diameter steel shaft the critical frequency calculated by FEM was 263 Hz, while the analytical result is 305Hz.

All the former considerations about the rotation speeds and critical rotation frequencies made this alternative solution seem unfeasible to support the rubber belt of the rolling road. However, given the necessity of having an alternative supporting solution for the rolling road's belt, the rolling cylinders concept was adapted to fit the rolling road system by reconsidering some of its design parameters. First, the operating speed of the rolling road was assumed as 80 km/h, in order to reduce the cylinder's rotating speed, and set it further from the critical one. Finally, the number of cylinders was reduced in order to be able to increase their diameter, which affect the flatness of the support but increases the critical speed value.

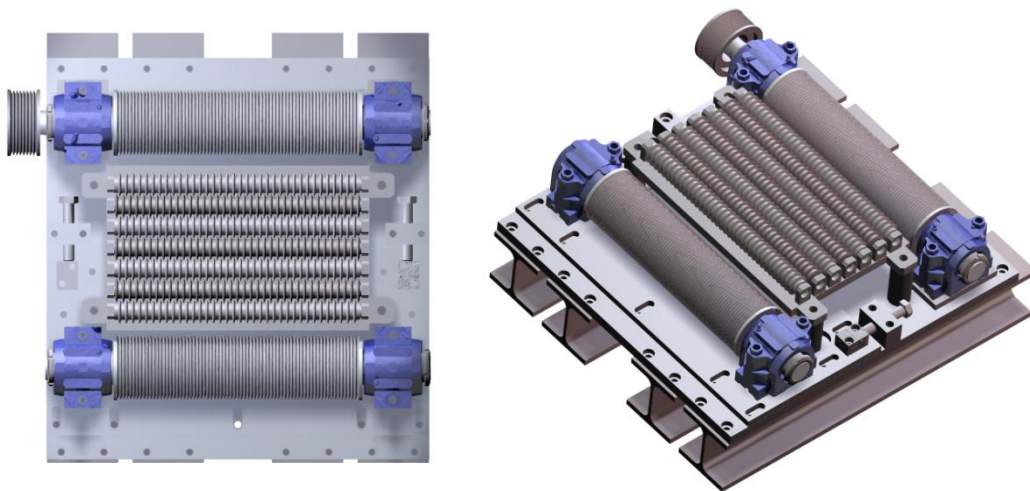


**Figure 46 - Rolling Road Support with 7 Rotating Cylinders**

By changing the rotating speed and varying the dimensions of the cylinders, different configurations were analyzed searching for a compromise between the critical speed and the diameter of the cylinders. The final decision was a cylinder with a diameter of 24.28 mm at the base of the ribs (34.5 mm at the top of the ribs) which has an analytical critical frequency at 394 Hz. As a reference, during the design process a 26 mm diameter shaft was analyzed with FEM, and a natural frequency of 386 Hz was found, which is accepted since we know the analytical formula overestimates the value. With the former dimensions, the

actual rotating frequency of the cylinders would be 291 Hz, and therefore the chosen diameter is adequate for the desired performance and works far from the critical speed.

With the bigger diameter supporting cylinders the number of them that could be fitted between the rolling road pulleys was reduced from 10 to 7. In the new situation, the center distance between the cylinders is 29.5 mm (instead of 23.5 mm) which still seems close enough as to provide a relatively flat support surface to the belt. Finally, some rolling bearings were chosen from the SKF product catalogue to support the cylinders according to the available space between them and the expected rotating speed. The most adequate were the deep groove single row ball bearings (61901-2rs1) having an internal diameter of 12 mm, an external of 24mm and a top speed of 19000 rpm. Figure 46 illustrates the final alternative concept to provide support for the rolling road's belt.

Though the concept works and its construction is feasible, other aspect must be considered for its implementation. Besides the risk of vibrations and whirling due to the high rotating speeds of the cylinders, the wear over the rubber belt also appears like an important concern for the implementation of the supporting cylinders system concept. We must consider that when considering the 7 cylinders and their ribs, the belt will be actually supported by the contact of the belt with the top of around 250 ribs. Since the supporting area is so small (created by the contact areas between the top of the cylinder's ribs and the belt), high stresses might arise causing a progressive damage to the belt. In this sense, the pneumatic support of the belt seems much more feasible, since the belt is homogeneously supported along the entire bearing's surface over which the fluid film is formed. Once again considering the small contact area supporting the belt, it is possible that slip will occur between the belt and the rolling cylinders, generating additional friction forces which will at the same time increase the belt's operation temperature, affecting its performance.

With the previous considerations and analysis, we may conclude that the alternative supporting system seems like a possible solution to provide support to the rubber belt. However, the cylinders will impose high stresses over the rolling road belt due to the direct contact between the belt and supports, which will considerably affect the life of the belt compared to the reference case of the air bearing support, were the reduced contact should maximize the belt's life. Besides, the implementation of the alternative system requires an additional speed limit decrease, which will affect negatively the testing parameters of the RuotaVia Test Rig.